JOURNAL OF RESEARCH of the National Bureau of Standards
Vol. 86, No. 3, May–June 1981

Contents

Library of Congress Catalog Card Number: 63–37059

For sale by the Superintendent of Documents, U.S. Government Printing Office.
Washington, D.C. 20402. Order by SD Catalog
No. C13.22/vol. 86(3). Single copy price $3 Domestic; $3.75 Foreign.
Subscription price: $13 a year; $4.25 additional for foreign mailing.

UNITED STATES GOVERNMENT PRINTING OFFICE, WASHINGTON: 1981

JOURNAL OF RESEARCH of the National Bureau of Standards
Vol. 86, No. 3, May–June 1981

An Intercomparison of Pressure Standards Between LNE and NBS

R. G. Driver*, J. C. Houck*, and B. E. Welch*

National Bureau of Standards, Washington, DC 20234

January 7, 1981

An intercomparison between a transfer piston gage used by the Laboratoire National d'Essais (LNE) and a primary standard piston gage of the National Bureau of Standards was performed over the range of pressure of 0.4 to 3.9 MPa. The agreement between the computation of the effective area of the LNE gage by the two laboratories was within 6.4 ppm and the agreement between the average of the pressures generated by these two gages was within 3.3 ppm, well below the estimated uncertainty of either gage (NBS 30 ppm and LNE 24 ppm).

Key words: Effective area; intercomparison; piston gage; pressure; primary standard; transfer standard.

An intercomparison of pressures generated by a transfer piston gage placed at the Laboratoire National d'Essais (LNE)'s disposal by the Bureau National de Metrologie (BNM) and by a primary standard piston gage of the National Bureau of Standards was performed at NBS over the pressure range 0.4 to 3.9 MPa.

The two gages differ somewhat in principle. The LNE gage is a simple piston and cylinder calibrated against a standard whose effective area is the average of the measured area of a piston and of a cylinder with theoretically calculated corrections of the pressure deformation of the piston and dilation of the cylinder. The NBS gage is a primary standard controlled clearance piston gage with the effective area derived from the measurement of the piston only, with an empirically determined correction based on the extrapolation of jacket pressure required to close the cylinder on the piston, and a theoretical pressure correction applied to deformation of the piston only. At the pressures at which this intercomparison was made, the pressure correction is small. At maximum pressure the fractional change in area for the LNE gage is 3.2×10^{-6} and for the NBS gage is -2.0×10^{-6}.

The NBS controlled clearance piston gage is gas operated with a piston of tungsten carbide with a diameter of 25.4 mm and a mating cylinder of tool steel. The effective area of the gage at 23 °C is $5.067819 \times 10^{-4} m^2$. The thermal coefficient of expansion of the carbide is 4.3×10^{-6}/°C and of the steel is 1.2×10^{-5}/°C so that the temperature coefficient of the effective area is 1.6×10^{-5}/°C. The change in effective area due to pressure is -5.07×10^{-7}/MPa.

The LNE piston gage is oil operated with a piston diameter of approximately 8.0 mm, and both piston and cylinder are tungsten carbide with a thermal coefficient of expansion of 4.1×10^{-6}/°C. The temperature coefficient of the effective area is 8.2×10^{-6}/°C and the pressure coefficient is 8.0×10^{-7}/MPa. The effective area at atmospheric pressure is $5.02724 \times 10^{-5} m^2$ at 20 °C.

The two gages and their connection through a coaxial capacitor gas/oil separator are shown schematically in figure 1. The interface between the oil used in the LNE gage and the dry nitrogen used in the NBS gage was monitored by a capacitance detector. This device [1][1] utilized the difference in dielectric constants between the oil and the gas to measure the height of the interface. This permitted adequate sensitivity to not only account for the hydrostatic head in the fluid but also to detect the small changes in level that are necessary for a rapid determination of the proper balance of the two gages.

The calculations for pressure measurements by both controlled clearance piston gages and simple piston and cylinder piston gages, as well as considerations of direct comparison, are given by Heydemann and Welch [2]. The two gages were set up with the oil/gas interface at the same level as the bottom of the LNE piston at its operating level.

*Center for Absolute Physical Quantities, National Measurement Laboratory.

[1]Figures in brackets indicate literature references at the end of this paper.

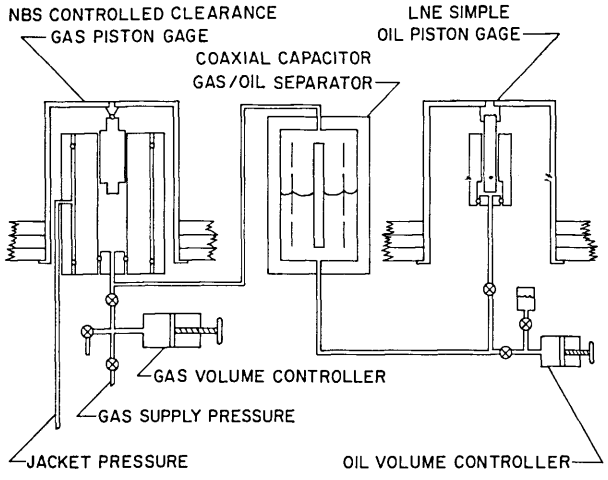

FIGURE 1. A schematic drawing of the two gages with the gas/oil separator.

A head correction (for nitrogen) was applied for the difference in level between the bottom of the NBS piston at its operating level and the level of the oil in the separator. The gages were operated at temperatures near 23 °C and the appropriate corrections were applied.

A total of 23 comparisons at 10 different pressures were made over a period of three days. One method of evaluating the data was the use of an NBS computer program for calculating the effective area of a piston gage to various orders of fits from the direct comparison of the test gage against a standard piston gage. The results of the lowest order FIT routine (F = PA) used for this gage give an effective area of the LNE gage of 5.027396 x 10^{-5}m² at 23 °C. This FIT routine gave three sigma of the calculation of the area to be 7.2 ppm of the area. The area of the LNE gage given by LNE is 5.027364 x 10^{-5}m² at 23 °C. This difference in area of the LNE gage determined by the NBS standard in this comparison with that given by LNE is 6.4 ppm in area.

Another method of evaluating the intercomparison was the calculation of the pressure generated by each piston gage according to the method used by the respective laboratories. The results of the 23 direct comparisons (the same points as used in the first method) are shown in table 1. The pressures were calculated for the pressure at the nitrogen oil interface. The average of the pressure calculated by LNE minus the pressure calculated by NBS is 13.0 Pa with a standard deviation of the mean of 5.8 Pa. The average of the pressure calculated by LNE minus the pressure calculated by NBS divided by the NBS pressure is 3.3 ppm with a standard deviation of the mean of 4.2 ppm. A plot of the differences in pressure calculated from the two gages versus the pressure is shown in figure 2. No quantitative explanation is given for the indicated systematic shift. It is due to using empirically determined non-smoothed values for the jacket pressure for zero clearance on the NBS gage. Using smoothed values for the zero clearance pressure removes the indicated shift and changes the calculated area by one ppm, much less than the estimated uncertainty of the gage.

TABLE 1. *Comparison of Pressures Generated by NBS and LNE in Chronological Order.*

Pressure by		Difference in Pressure	Difference in Pressure
			Pressure
NBS (Pa)	LNE (Pa)	LNE-NBS (Pa)	LNE-NBS / NBS
389874.6	389858.1	−16.5	−42.3 x 10^{-6}
1169566.0	1169562.2	−3.8	−3.3 x 10^{-6}
1949227.0	1949266.5	39.5	20.3 x 10^{-6}
1949232.0	1949266.3	34.3	17.6 x 10^{-6}
2728940.0	2728969.1	29.1	10.7 x 10^{-6}
3508676.0	3508670.9	−5.1	−1.5 x 10^{-6}
3898543.0	3898521.7	−21.3	−5.5 x 10^{-6}
3898569.0	3898538.9	−30.1	−7.7 x 10^{-6}
3118814.0	3118829.3	15.3	4.9 x 10^{-6}
2339075.0	2339119.9	44.9	19.2 x 10^{-6}
1559369.0	1559412.9	43.9	28.1 x 10^{-6}
779713.8	779708.7	−5.1	−6.5 x 10^{-6}
389872.8	389858.4	−14.4	−37.0 x 10^{-6}
389868.0	389859.5	−8.5	−21.9 x 10^{-6}
1559379.0	1559415.0	36.0	23.1 x 10^{-6}
1949227.0	1949270.5	43.5	22.3 x 10^{-6}
2339080.0	2339120.1	40.1	17.2 x 10^{-6}
3898543.0	3898528.1	−14.9	−3.8 x 10^{-6}
3898557.0	3898531.6	−25.4	−6.5 x 10^{-6}
2339081.0	2339120.9	39.9	17.1 x 10^{-6}
1949225.0	1949269.0	44.0	22.6 x 10^{-6}
1559372.0	1559413.3	41.3	26.5 x 10^{-6}
389865.0	389858.3	−6.7	−17.1 x 10^{-6}
Average		13.0	3.3 x 10^{-6}
S.D. of the mean		5.8	4.2 x 10^{-6}

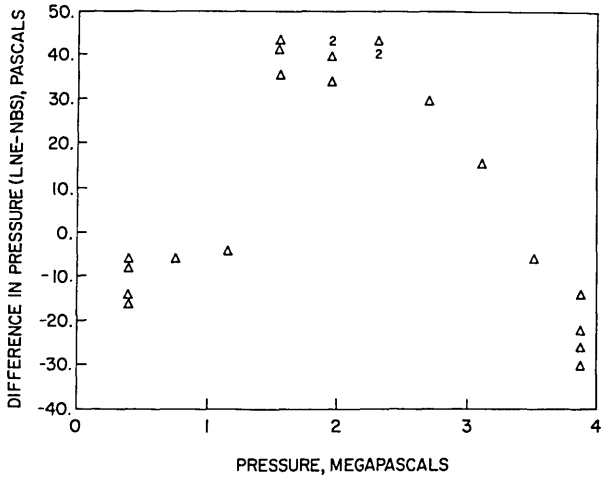

FIGURE 2. Plot of differences in pressure computed by LNE and NBS versus pressure.

Both methods of expressing the results of the intercomparison show significantly better agreement between the two gages than the estimated systematic uncertainty of either gage (NBS 30 ppm and LNE 24 ppm). The differences observed, 6.4 ppm by area comparison and 3.3 ppm by pressure comparison, indicate that the two different methods of calculating effective areas are well verified at this pressure range.

We thank R. Touzin and J. C. Legras of LNE for their participation in the intercomparison.

References

[1] Tilford, C. R.; Martin, D. A high sensitivity gas/oil pressure separator, to be published in R.S.I.

[2] Heydemann, P. L. M.; Welch, B. E. *Experimental thermodynamics.* Vol. II Chapter 4, Part 3. Piston Gages, Editors: LeNeindre and Vodar, Butterworths 1975.

JOURNAL OF RESEARCH of the National Bureau of Standards
Vol. 86, No. 3, May–June 1981

Foundations of Metrology

John A. Simpson*

National Bureau of Standards, Washington, DC 20234

January 7, 1981

The theory of measurement has attracted the attention of a number of philosphers whose works remain largely unknown to metrologists. Recent work in the development of Measurement Assurance Programs has demonstrated the power of this theory as a tool for guiding the development of measurement systems. The elements of the theory, especially that of Carnap and its applications to metrology, are developed as an aid to program planning and evaluation.

Key words: Epistemology; measurement; measurement assurance; metrology.

1. Introduction

Metrology is defined as the science of measurement, and if broadly construed would encompass the bulk of experimental physics. The term is usually used in a more restricted sense to mean that portion of measurement science used to provide, maintain, and disseminate a consistent set of units or to provide support for the enforcement of equity in trade by weights and measurement laws, or to provide data for quality control in manufacturing.

In this restricted sense metrology has taken on the nature of an art or craft rather than a science, and has attracted little academic interest. As a consequence its literature, although extensive, tends to be of an *ad hoc* character, is widely scattered, and appears mainly in the form of reports or internal documents. There exists no extensive systematic treatment of the subject comparable to the great texts of other disciplines. However, the subject does have an internal logical structure, one version of which has been articulated at NBS over the past two decades as the concept of Measurement Assurance Programs has been developed and applied to measurement services.

While presenting in some detail this version, our treatment does not aspire to be a definitive text but rather to provide an overview of the subject to give those responsible for managing organizations active in metrology a conceptual grasp of the subject sufficient for intelligent program planning and evaluation. Because of the background of the author the few examples given will generally be taken from the field of mechanical metrology; but the principles illustrated are task independent.

*Center for Mechanical Engineering and Process Technology, National Bureau of Standards.

2. Context of Measurements

A measurement is a series of manipulations of physical objects or systems according to a defined protocol which results in a number. The number is proported to uniquely represent the magnitude (or intensity) of some quantity[1] embodied in the test object. This number is acquired to form the basis of a decision effecting some human goal or satisfying some human need the satisfaction of which depends on the properties of test object.

These needs or goals can be usefully viewed as requiring three general classes of measurements.

1. *Technical:* This class includes those measurements made to assure dimensional compatibility, conformation to design specifications necessary for proper function or, in general, all measurements made to insure fitness for intended use of some object.

2. *Legal:* This class includes those measurements made to insure compliance with a law or a regulation. This class is the concern of Weights and Measures bodies, regulators and those who must comply with those regulations. The measurements are identical in kind with those of technical metrology but are usually embedded in a much more formal structure. Legal metrology is much more prevalent in Europe than in the United States, although this is changing.

3. *Scientific:* This class includes those measurements made to validate theories of the nature of the universe or to suggest new theories. These measurements, which can be

[1] For our purposes we adopt the B. Ellis [1][2] definition of a quantity. A quantity is a kind of property that admits of degrees, and which therefore is to be contrasted with those properties that have an all or nothing character (for example, being pregnant).

[2] Figures in brackets indicate the literature references at the end of this paper.

called scientific metrology, properly the domain of experimental physics, present special problems and will be dealt with only briefly at the end of this paper.

The path of reasoning between an identified goal or need and the measurement to attain that goal is a thorny one. Many valid measurements do not result in useful information. The property measured often does not adequately predict the fitness for use. Often quantities for measurements are chosen for their convenience rather than their importance. The metrologist is seldom in a position to do much about this unfortunate state of affairs. This problem is the concern of the design engineer, the regulator, the Quality Control Manager, or in brief, the decision maker. Supplying the decision makers with the most reliable numbers characterizing the properties they have designated, in the most economical manner, is all metrologists can do in their professional capacity.

This task, although limited, is a worthy one requiring all of the ingenuity, knowledge, and professionalism one can muster. It is a two-fold task: one must generate a measurement system, which in the NBS view is a *production system* whose product is numbers, and a *quality control system* to confirm the validity of those numbers [2].

The first of these tasks is an engineering hardware problem while the second is largely a software management problem. The software consists of record keeping, reporting, qualification, and similar activities often depending heavily on statistical mathematics. We will deal with each in turn.

3. Elements of a Measurement System

There are many ways of enumerating the elements of a measurement system since it consists of these eight elements, combined in more or less complex groupings:

Physical Concepts
Physical Laws
Instruments
Standards
Human Operators
Procedures
Environments
Computations

It has proved useful over the years to group these elements under two general headings: *Properties of the Investigated Object*[3] and *Properties of the Measurement Algorithm* where the *Investigated Object* is the subject to be measured and the *Measurement Algorithm* includes all means and procedures used to produce the desired number. This grouping is useful for identifying sources of error and for remedial action when such are discovered. The procedures for successfully accomplishing such action differ markedly depending on the grouping in which the faulty element lies. This important fact seems to have first been recognized by Volodreskii [3].

3.1. The Role of the Investigated Object

The investigated object (henceforth shortened to object) plays two essential roles in a measurement system: it must embody the quantity of interest and it must generate a signal to which the measurement algorithm can respond. This signal must be unambiguously related to the magnitude or intensity of that specified quantity. Knowledge of the relationship between the quantity and the signal requires a model of the object. This model is based on the laws of physics or our understanding of the universe. It is usually a software model, and equation or the like which quantitatively predicts the signal as a function of the quantity to be measured. Unfortunately, objects have complex natures and hence seldom are perfect embodiments of single quantities. For example, the Kilogram of Paris embodies a specific volume as well as the unit of mass: a standard cell is not a "pure" voltage source but rather such a source in series with a non-linear complex impedance. Moreover the magnitude of the quantity of interest in the object may itself be a function of environmental parameters not of immediate interest. The length of a material body, say a gage block, is intrinsically a function of the temperature of that block. The model must include all relevant properties of the object.[4]

The model must also predict the signal that is to be used to drive the measurement algorithm. This signal is almost invariably a quantity which differs in nature from the quantity to be measured. For example, the beam of the common balance used in mass determinations responds to a force signal generated by gravity operating on the mass of the object in the pan. Many objects generate more than one signal that could be used for measurement. A gage block as an embodiment of length, can, if the measurement algorithm is a caliper, generate a force signal as the jaws close on the block, an optical signal, if measured by an interferometer, or an electrical signal, if used in a capacitance arrangement. Any of these signals can be and are used, the choice being made on considerations of convenience or current state-of-

[3] The investigated object may in fact be a complex system with internal structure but for purposes of this discussion the word object has the advantage of compactness of expression and no generality is lost.

[4] What constitutes a relevant parameter is a problem that has attracted philosophical attention, Rudolph Carnap [4], for example. In practice, except at the highest levels of scientific metrology, enough is known about the object that identification of the relevant parameters is easy; in any event, if one parameter is overlooked the resultingly high observed uncertainty of the measurements will soon call this fact to one's attention.

the-art in measurement algorithm development. While this signal redundancy makes life simpler, the fact that most signals are generated by several quantities embodied in the object makes life at times difficult. For example, the force signal generated by the mass of an object on a balance pan is contaminated with a signal identical in kind generated by the buoyant force of the air displaced by the object's volume. This particular problem has recently given the mass community problems [5, 6]. In length metrology the fact that the distance between the apparent reflection planes (the optical length) of a gage block depends both on the length of the block and the complex dielectric constant of the material remains an unsolved problem limiting among other things work on absolute density.

The signal, besides being impure, may also be a function of environmental parameters even if the quantity itself is not. A case in point is the dependence of gravity force generated by a mass on the value of the local acceleration of gravity; here, then, the signal is a function of location while the mass is not.

More generally the nature of the object can be expressed as a matrix where the rows are all the physical quantities embodied in the object while the columns are the all of the signals generated by that object. An ideal object would be one in which the matrix was diagonal, in the sense that for every quantity there would be one and only one signal. No such object exists. The proper treatment of the off-diagonal terms is one of the central problems of metrology. We shall return to this problem in section 4.

In any event the first step in constructing a measurement system is to reduce the object to an idealized model which represents those properties or attributes believed to be germane to the intended measurement, i.e., those which satisfactorily predict the signal as a function of the magnitude or intensity of the desired quantity. For example, a gage block may be modeled for a force-based algorithm as an impenetrable rectangular parallelpiped characterized by a single length between its gaging surfaces. However, in this case the model is too simplified for most purposes, and current models include the fact that length is a function of temperature, that the block is elastic, deforming on contact, and that the faces may be non-parallel. Thus, the model may be simple or complex, where complexity and desired accuracy go hand in hand, but the model only weakly reflects the measuring system by being required to predict the signal to which the chosen measurement system responds. The converse is not true; the measurement system reflects the model strongly since it must provide all of the parameters necessary to permit the model to predict the quantity from the observed signal or signals. Hence, generally a more complex model will call for a more complex measurement system measuring a greater number of properties of the object or of the environment.

The model is never complete or perfect and the difference between the model and the real properties, including the signal expected, is called *model ambiguity*. The model ambiguity sets a lower limit on the uncertainty of the measurement since below this level the object is not in fact fully defined. In more complex objects this model ambiguity is most often the dominant uncertainty term; an example that comes to mind arises in screw thread metrology where a measured quantity, flank angle, implies a model in which the thread flanks are planes. In practice, when dealing with carefully gound thread gages, this model is useful. However, in fasteners made by use of a die or a roll, the flanks most definitely are not planes, and flank angle loses its meaning.

Model ambiguity is a particular type of systematic error which exists if the measurement algorithm is flawless. Failure to recognize this fact can lead to major wastes of resources since no improvement in the measurement algorithm can reduce this error. No amount of research on precision balances will reduce the inconsistencies of the mass scale caused by air buoyancy correction problems. Model ambiguities are the source of the vast majorities of measurement inconsistencies which can only be reduced by improvement of the model.

Given that a certain condition is satisfied there exists a strategy which can reduce model ambiguity identically to zero. This strategy uses objects called variously "prototypes," "artifact," or "gold plated" standards and, in effect, takes a particular object and defines it to be its own model. This amounts to saying that this particular object is the perfect and complete realization of the class of objects to which it belongs and hence the model ambiguity is, by definition, identically zero. The condition to be satisfied is that all objects to which the standard refers must be essentially identical to the standard both in kind and in degree. For example in mass, the only SI unit still using this strategy where the Paris Kilogram is the kilogram of mass, the only objects where mass can be unequivocally defined are one kilogram weights made of platinum. All other objects differing in size or material have masses that can only be approximated (admittedly to a high degree) by comparison with the kilogram. The strategy has the further disadvantage that if the prototype is lost, destroyed, or changed in value, all objects of its class must be recalibrated. In principle, if someone drops the Paris Kilogram, every scale in the world would be out of calibration the instant it hit the floor.

However, lower down the measurement hierarchy the strategy works well; for example, the American Petroleum Institute pipe threads, where sets of "gold plated" gages kept at NBS and other National Laboratories can be compared to almost identical working gages by algorithms much simpler than those required to compare a gage to a drawing. The problem of extensibility, i.e., using a two-inch gage to calibrate a three-inch gage never arises and the

gages are so close to identical that functionally no harm is done by replacing a worn or broken gage by the last good gage and carrying on. For highly derived or complex objects, gears are another example that comes to mind. The possibility of using this ploy should always be explored since it is extremely efficient in those cases where it can be used, even though it requires a separate standard for each and every size of a class of objects.

In the search for model ambiguities it is often possible to use a measurement algorithm known from another context to be error free (at some level of accuracy) to measure the object. In this case the total uncertainty can be ascribed to the model ambiguity. The use of high precision optical interferometry to read caliper jaw movement when checking for the correction due to the elastic deformation of the object under the force of the caliper jaws is an example. Optical interferometry can, for this purpose, be considered error free.

4. The Measurement Algorithm

In our classification, the measurement algorithm includes everything involved in the measurement except the object and the final number. It includes the instruments used, the protocols followed, the characteristics of the human operator, the calculations made and the environment in which they operate. In brief it is the "factory" whose raw materials are objects and whose product is numbers. Just as in the case of the object we must have a model of this "factory" which predicts how it treats the signal from the object, processes it, and generates the number. To be fully satisfactory the model must account for the effects of environment on this process and, most importantly, predict how it "loads" the object signal source and hence affects the relationship between the quantity and the signal of the object. Neglect of this factor, typified by using a low impedance voltmeter on a high impedance source or using a high force caliper to measure the diameter of an egg, leads to gross errors.

The process, if it is to be useful, must generate numbers which have certain properties. These properties arise out of our expectations concerning them. We would like to use them as surrogates of measurement, i.e., once they are obtained for a stable object we would like to use them to avoid measuring the object at a future time or a different place. Prepackaged food is a clear example where the scale in the manufacturing plant virtually eliminates weighing in every store. However, to accomplish this goal we must be assured that, within some predetermined uncertainty, every competent metrologist with suitable equipment at any different point in the space/time continuum would assign to the same object the same numbers representing the same quantity that we did. When we have accomplished this often difficult feat we say we have a *proper measurement algorithm* and our numbers are *proper measurements.*

The concept of properness is a generalization of the concept of precision or reproducibility often used by writers on measurement. We prefer the more general term since it is often not clear whether the authors refer to the spread between successive repeated measurements, between runs, between measuring stations, or between laboratories. With properness you are assured you are working with worse-case figures.

Before we discuss the details of the measurement algorithm and how we accomplish a proper measurement, we must examine some general principles which allows us to define in broad generalities what constitutes a "competent metrologist with suitable equipment." Our guidance in this case comes not from the theory of physics but from philosophy. Rudolph Carnap and similar thinkers [1, 4] have articulated the requirements of any measurement algorithm which is to yield proper measurements. They also simultaneously determine the minimum *a priori* information that a metrologist must have in order to be competent to duplicate another's measurement.

Although based on Carnap, what follows is a modification in detail of his exposition and somewhat an extension. It may be called the NBS school. The differences will not be explained in detail, only noted in passing. The position starts from an operational point of view and considers that every measurement algorithm defines the quantity measured.[5]

Our position is that, for example, interferometry defines the optical length of a gage block and a caliper defines its mechanical length. These lengths are separate and distinct properties of the block and logically unrelated. One arbitrarily chooses which length to measure on grounds of intended use or convenience. In this view, optical length and mechanical length are not imperfect measures of "true" length but independent quantities of full stature each in its own right. The question of "true" length is considered moot since it cannot be decided upon by a "true" measurement algorithm. Obviously such a posture gives rise to problems in the relationship of measurement to experimental physics, some of which will be touched on later;[6] however, in technical or legal metrology, since all the different lengths are in fact within less than a micrometer of being the same, it is perfectly practical to adopt this non-judgmental point of view.

For any such length or other quantity, a competent metrologist with suitable equipment is one who has a realization of four axioms.

---

[5] This position is closer to P. W. Bridgeman [7] than to Carnap who takes a more expansive view, including an operational definition as only one element. For a contradictory position, see H. C. Byerly and V. A. Lazara [8].

[6] For treatments of these difficulties, see Byerly and Lazara, op. cit. or Ellis, op. cit.

1. Within the domain of objects accessible one object must be the unit.

2. Within the domain of objects accessible one object must be zero.[7]

3. There must be a realizable operation to order the objects as to magnitude or intensity of the measured quantity.

4. There must be an algorithm to generate a scale between zero and the unit.[8]

To make the above clear, consider the following system:

> The quantity of interest, temperature;
> the object, a human body;
> the unit, the boiling point of water 100°;
> the zero, the triple point of water 0°;
> the ordering operator, the height of a mercury column in a uniform bore tubing connected to a reservoir capable of being placed in a body cavity;
> the scale, shall be a linear subdivision between the heights of the column when in equilibrium with boiling water and water at the triple point.

This is a well-known system the properness of which is the basis of medical diagnosis.[9]

Once a measurement has been made the test for competency stiffens and all other metrologists to be considered competent must have the identical realizations of the axioms.

The essence of designing a measurement algorithm capable of making proper measurements is choosing realizations of these axiometric operators which are capable of independent replication by the universe of metrologists interested in the measurements.

For certain parts of the task one has a great deal of help. The Treaty of the Meter sets up an international structure of various organizations, including the International Bureau of Weights and Measures, charged with defining units for additive quantities and both units and zeros for nonadditive quantities. The International Bureau also disseminates such units by "prototype standards" (Kilograms Numbers 4 and 20 for the U.S.) or prescriptions such as those for the realization of the Kr^{86} standard of length or the Cs second. Many other standards groups do the same for highly derived standards such as pipe gages from the American Petroleum Institute.

The zero units for extensive quantities are usually commonly agreed upon as null objects such as no mass on the balance or a short circuit (beware of thermal voltages) on a voltmeter.

The scale generation usually does not become a matter of controversy in the practical world although many have suggested it plays a central role in scientific metrology.[10] Whether to adopt 212 or 100 degrees between fixed temperature points or to divide an inch into thousandths or 25.4 mm can usually be worked out between metrologists.

The crux of most cases of improper, or allegedly improper, measurements, lies in the ordering operator. There are very few operators which have the authority of an international or national standards body. ISO has defined the ordering operator for gage blocks but not, for example, for ring gages. A cylinder, if it is used as a gear or thread wire, has a defined ordering operator but has none if it is a plug gage or the piston of a deadweight pressure generator. Decades of controversy surround the ordering operator, actually the much simpler equality operator (a special case of an ordering operator), for threaded fasteners.

The philosophers of science give little guidance on the process by which the metrologist makes the choice between all possible measurement algorithms which can be developed to satisfy the measurement axioms. Carnap sums up the total guidance as follows:[11]

> "We thus have a genuine choice to make here. It is not a choice between a right and wrong measuring procedure, but a choice based on simplicity. We find that if we choose the pendulum as our basis of time the resulting system of physical laws will be enormously simpler than if we choose my pulse beat. —This simplicity would disappear if we based our system of time measurement on a process which did not belong to a very large class of mutually equivalent processes."

Leaving aside the question of what is a simple law and how one establishes mutual equivalency without a preconceived measurement process, this advice is not particularly helpful to the practicing metrologist. What, if any, effect on physical laws a particular definition of, say, flank angle on a screw thread or specific rotation of a sugar solution for customs regulation, can be expected to have is at best obscure. There is even less help available as to how the model of the algorithm chosen is reduced to practice, i.e., hardware and protocols. To usefully attack this problem it is necessary to introduce the concept of *limited properness*.

[7] The criteria outlined here are suitable for all physical quantities and are the most general ones. For those quantities for which an addition operation can be defined a simpler set of three axioms is possible. However, measurement systems built on additivity are awkward in practice and even in mass where a particularly simple addition operator is available the least significant digits are obtained by use of a four axiom system. Gage blocks were an attempt to utilize an addition operation system but modern practice calibrates them by four axiom methods although the addition operator is important in their practical use.

[8] These operators must satisfy certain formal requirements as to symmetry, transitiveness, etc. For details see Carnap, op. cit., Chap. 6.

[9] There are some problems relating it to fundamental concepts, see Ellis, op. cit., Chap. VI.

[10] See Ellis, Byerly, previously cited works.

[11] R. Carnap, op. cit., chapter 8

All measurements taking place in the real world exhibit an intrinsic limited properness in that equality between reproduction will always have an uncertainty whose lower bound is either Johnson (kT) noise or that set by the Heisenberg uncertainty principle. Few measurements in technical or legal metrology approach either limit. The more important limits of properness are under the control of the metrologist and are those introduced by adopting a model for the object or the algorithm which is known to be imperfect. The governing principle is to pick the measurement system where the total measurement uncertainty can be demonstrated to be less than, but not wastefully less than, the uncertainty needed by the decision maker. It makes little sense to measure the dimensions of ceiling tile by laser interferometry when the decision to be made is whether or not the joints will appear straight to the naked eye.

There are several distinct manners in which the economies inherent in limited properness can be realized. The most frequently used manner is to restrict the class of objects "suitable" for measurement. An excellent example is the detailed design specifications applied to weights used in trade. By restricting the material, and hence the density, it is possible for legal metrology purposes to simplify the measurement algorithm and, for instance, eliminate an explicit air buoyancy correction. Such a procedure appears a direct violation of the Carnap formal requirement that all operators satisfy a connectedness property, that in the domain of the quantity M any object a or b which has M is either equal in M or one has less M than the other. What has been done in introducing the concept of "suitable" is to redefine what we mean by *any object*. Little damage to the logical structure results from such a choice.

A second choice is to limit the environmental conditions under which the measurement can be implemented. The length metrologists' insistence on 20° C working environment is an example of this way of simplifying an algorithm, or perhaps more succinctly, of restricting the universe.

The third strategy which can be used is to limit the range of magnitude to be covered.[12] This is popular in the temperature field where more than two fixed points have been defined and different interpolation algorithms are defined between pairs of them. All such strategies should be explored before a choice of measurement systems is finalized.

After a preliminary choice is made, it is useful to analyze the system for sources of uncertainty. This analysis is useful only if the object's model ambiguity has first been determined. Uncertainties or errors can enter at any of the realizations of the axioms.

There may be a unit error, a scale error, or a comparison error. Each of these errors can arise either because the realization is imperfect or, more frequently, because the realization has not been described in sufficient detail that the concerned "competent metrologists" have been able to effectively replicate it. The first of these causes can be attacked by high quality engineering, making use of all that is known of instrument design [9], properties of materials and precision workmanship and by a generalized form of experimental design.

There are three basic strategies to accomplish error control by design of the measurement which have developed over the years and which can often provide a useful conceptual framework within which to attack a given problem. The strategies deal directly with the basic problem that both the models of the object and of the candidate algorithm have to contend with mixed (non-single quantity) signals and responses, or in our matrix formalism, off-diagonal terms. For concreteness, let us consider the measurement of the x, y coordinates of n points in a plane by use of a two-axis measuring machine. The ideal situation would give a set of idealized observational equations as follows:

$$\begin{aligned} x_i &= k\hat{x}_i \\ y_i &= k'\hat{y}_i \end{aligned} \tag{1}$$

where x_i and y_i are the true coordinates, i.e. in a coordinate frame attached to the workpiece, $\hat{x}$ and $\hat{y}$ are the x and y axis scale readings of the machine and k and k' are the invariant scale constants of the machine which implicitly contain the unit.

Unfortunately, machines are not geometrically perfect and if the x and y axes are not orthogonal the observational equations will develop off-diagonal, or coupling, terms, i.e.

$$\begin{aligned} x_i &= k\hat{x}_i + \alpha\hat{y}_i \\ y_i &= k'\hat{y}_i + \alpha'\hat{x}_i. \end{aligned} \tag{2}$$

If the axes are curved or Abbe angle errors exist, the equations become still more complex

$$\begin{aligned} x_i &= k\hat{x}_i + \alpha\hat{y}_i + \beta\hat{y}_i^2 + \ldots + \gamma\hat{x}^2 + \ldots \\ y_i &= k'\hat{y}_i + \alpha'\hat{x}_i + \beta'\hat{x}_i^2 + \ldots + \gamma' y^2 + \ldots \end{aligned} \tag{3}$$

where the γ-like terms reflect scale nonuniformities. In a measuring machine with a screw for reference, they might well be written in sine form to characterize periodic errors.

In general, all of the coefficients are functions of temperature and hence, if the temperature changes, become functions of time with various time delays. The problem of

[12] Support for this strategy is implied by Carnap, op. cit., chapter 10

algorithm design is to find optimum ways of dealing with the n equation array of eq (3).

Three general strategies have developed. The first, called by J. Bryan, "brute force," is to develop auxiliary or test algorithms which measure the off-diagonal terms and then to reduce them by "reworking" the machine (algorithm) until they become insignificant. The machine is then treated as "perfect," and equations of type 1 are used for the measurement. Since the implementation of the auxiliary algorithms is, of necessity, spread out over a long time compared to the time for a single measurement, temporal stability is of critical importance and, hence, leads a legitimate emphasis on temperature control.

A second strategy, which might be called "correction," is to measure in auxiliary or test algorithms the off-diagonal terms and then either by analog devices on the machine, i.e., compensator bars, or by computation, render them harmless. Note that, for example, eqs (2) become linear and much easier to deal with if α is a constant and not a variable unknown. If the off-diagonal terms are allowed to remain large, the stress put on the temporal stability is even more severe than in the "brute force" technique where the coefficients are forced to be negligible in size. Failure to provide this temporal stability by adequate temperature control probably accounts for the historical failure of this technique. Another difficulty with this approach is that it is difficult to derive auxiliary algorithms which measure the desired coefficients directly and these coefficients tend to be complex combinations of the auxiliary scale readings. The strategy moves the problem to the auxiliary system where it may or may not be easier to solve. For example, on the three-axis measuring machine, α is a combination of axes nonorthogonality, y roll and the y axis arm length. In three dimensions α becomes, moreover, a function of z. Multi-parameter factors are difficult to deal with in the analysis. A major advantage of the "brute force" technique is that any combination of negligible quantities is negligible and, hence, the detailed dependence of the coefficients on the auxiliary quantities need not be worked out.

The third strategy and the one currently being explored at NBS is a conceptually straightforward attempt to solve eqs (3) in all their complexity. It has been called a Redundant Algorithm because the coefficients (k, α, etc.) as well as the variables (x_i, y_i) are treated as unknowns. There must be many more observational equations, and hence, measurements, than the "n" variables the algorithm sets out to measure. Looked at another way, all of the measurements which are auxiliary in the other schemes are lumped together with the desired measurement into a single procedure. The measurement need not be redundant in the statistical sense.

The greatest advantage of this attack is that the "calibration" of the machine occurs simultaneously with the measurement instead of days, weeks, or months apart, and the question of loss of calibration by misadventure cannot occur. For instance, the "four points in a plane" algorithm we have tested takes about one hour to perform. It consists of measuring the x, y position of four points on a plane repeated with the plane rotated approximately 90°. It accomplishes the auxiliary measurements, an "absolute" calibration of a rotary table at 90° increments, and a measurement of the orthogonality of the machine axes. There are, in fact, sufficient measurements taken to determine in principle 24 coefficients. This telescoping in time greatly reduces the demands on the temporal stability of the machine, especially since that portion of the drift in each coefficient which is linear with time can be eliminated relatively simply by the introduction of more explicitly time-dependent coefficients. This particular ploy has been used successfully in our gage block laboratory for a number of years.

The comparison of methods cannot be complete, however, without a discussion of the different manner in which the second part of the reported number, the error estimate, is obtained. The error estimates reflect a considerable difference in philosophy, although both the "brute force" and "correction" strategies divide the error into two parts, a "random" and a "systematic." The random component is obtained by repeating the measurements, both prime and auxiliary, a number of times, and inferring the variance around the mean by the rules of elementary statistics. The systematic component is in the "brute force" method bounded by a "worse case" calculation based on the residual values of the off-diagonal terms after the machine has been refined to its current state. This results in a conservative estimate of the error in most cases. It is essentially this calculation which defines the term "insignificant" as a goal for machine correction. An insignificant fault is one whose maximum possible effect on the measurement is less than some limit set by end-use of the measured object.

There remains a danger, which may be remote, but to which most metrologists have fallen victim. This danger involves what one may call hidden coefficients; these are variables which affect the measurement but which are not modeled by the observational equations. For example, suppose one neglects temperature change in a gage block measurement. The protection against such an oversight is redundancy by repeating the measurement, averaging, and observing the deviation from the mean which will reflect this temperature drift if it is significant alert the metrologist. As has been so often pointed out, the "random" variations of metrology are seldom random in the statistical sense, but reflect a wider spectrum of ills, the change of an unmodeled parameter being foremost among them. This protection achieved by averaging is far from absolute since in the limited period of the measurement the critical

variable may not change, as it might at some future time, but the protection is nonetheless helpful. To obtain this limited help, the redundance must "span" the measurement in question. Where there are gaps, as in the time between the "calibration" and "use" of an instrument, this assurance is missing. Any super-redundancy, i.e., statistical redundancy beyond that needed to characterize all parameters of the model, introduced into a redundant algorithm spans the complete process and avoids this trap. Note also that in this scheme, there is no separation of "random" from "systematic" and the indices of fit derived from the massive least squares solution of the now overdetermined equations are the "metrologically random" errors of the complete measurement process. They reflect not "worse case" but the case that existed over the range of parameters used in that particular measurement.

The use of a single massive least squares adjustment has another advantage which arises from the peculiar nature of the coefficient k. This coefficient of the principal diagonal term introduces the unit into the measurement and, hence, has a special importance. The unit while vital to the measurement cannot be checked by the usual forms of redundancy since the laws of the universe operate independently of the units in which they are expressed. The reverence in which "standards" are held reflects their critical nature. In a super-redundant algorithm the unit may be introduced at several points in an independent, i.e., truly redundant, manner. For example, in our gage block algorithm it is entered in the comparator constant k and in the difference x_1-x_2 of two masters. This provides a check of x_1, x_2, and k which is difficult to obtain in any other way and provides further protection against mistakes.

The "correction" strategy is similar in principle to the "brute force" in its treatment of errors except, in this case, it is possible in theory to calculate the "actual" rather than the "worst case" systematics.

At this point we can begin to see the relative advantages of the different strategies and types of measurement programs to which they are most adapted.

The "brute force" technique requires a large initial "capital" investment in characterizing the machine over its entire working volume on a "does not exceed" basis. Also required is the establishment of an environment, both physical and procedural, that assures the maintenance of this level of performance over a "longish" time span. Depending on the requirements on accuracy, an investment in machine upgrading may also be required. However, once these conditions are met, production runs are rapid, simple to perform, and any workpiece within the machine's capacity can be characterized on a valid "maximum deviation from nominal" (tolerance) basis. It is obviously advantageous where the piece part tolerance is significantly larger than machine tolerance or where the part has a model ambiguity which is large, i.e., the piece is complex or only moderately well characterized. I would expect that the products of high precision industry lie in this class of objects.

The super-redundant strategy on the other hand requires little or no investment in machine characterization. It does, however, require a considerable investment in computer programming which is applicable to only one narrow class of objects. Moreover, the "production" runs will inevitably be more time consuming since calibration time is not spread over more than a single measurement. It does, however, offer the promise of higher ultimate accuracy since the machine needs only short-term repeatability. It also offers rigorous characterization of precision and accuracy of the values obtained.

It is advantageous in those instances where comparatively few types of workpieces are measured but where the measurements are required to be the absolute "best" in terms of accuracy and confidence in that accuracy. This requirement, of course, implies that the workpieces are simple enough in form and high enough in workmanship that the model ambiguity warrants such measurements. This workload is characteristic of the master gages with which NBS deals.

The "correction" strategy requires an inordinate capital investment in complete functional machine characterization and extensive computation on outlay which would only be justified if the brute force method was insufficiently accurate while simultaneously the workload was too heavy or diverse to make the super-redundant approach feasible. I know of no such circumstances other than when the scale of the workpieces becomes so large that measuring machine accuracy is extremely difficult to achieve, as in the aircraft industry, shipbuilding, or heavy ordnance.

Regardless of the strategy adopted there remains the problem of transferring the measurement algorithm to all interested metrologists. This communication problem is attacked largely through the voluntary standards community where measurement algorithms can be institutionalized and disseminated widely as test methods or recommended practices. The process of adoption of standards can be painfully slow.

5. Measurement Quality Control

Measurement quality control starts as soon as the first measurement is made. The principal tool for the metrologist is redundancy. One repeats the measurement on a stable object and compares each successive measurement with the set of all measurements. It is typical of all real systems that there will be a spread in values. Statistics tell how to derive indices of precision (reproducibility) for each system. The goal is to produce a series of values which demonstrate a

stable[13] mean and a random distribution around that mean. When this situation is achieved within a single run, within-group statistical control is said to be achieved. But this within-group control is not enough; the same statistical control must be achieved between runs, between *measurement stations* within the initiating laboratory, and finally between all competent metrologists. Only after this task is accomplished can one have assurance of a proper measurement system turning out proper measurements.

Over the years a number of institutionalized aids have developed for the process of obtaining properness of measurements and the maintaining of this quality over time. The first of these institutions to develop addressed the detection and elimination of the unit error, one which seems to have dominated in earlier times. The institution is still dominant in weights and measures, and in legal metrology in general.

This institution is a calibration network where stable artifacts, often realizations of units, are sent to a different location where a "higher" artifact or unit is maintained. Working standards are "calibrated," i.e., compared with a similar object, often a secondary standard which in turn had been compared with a national primary standard and so on up the line. Since the artifacts are almost identical, model ambiguities are low and when returned to its original site the artifact provides both a source of the unit and often a one-point check of the total system. For simple, stable objects, the system has some virtue, especially if two or more calibrated objects can be used to provide an independent, even although only one point, system check.

This calibration scheme gave rise to the concept of measurement traceability [10] which wrote into contracts the requirement that such a chain be established. The system has some shortcomings:

1. it requires a stable non-ephemeral artifact;
2. it requires a measurement robust against environment;
3. it is expensive if artifact is large, fragile or complex;
4. it provides at best only a one-point check of the system; and,
5. it focuses on the quality of means of measurement rather than the measurements themselves.

To deal with cases where no stable artifact exists or where it is ephemeral in the sense that the accepted measurement algorithm is destructive, the concept of a Standard Reference Material was developed. Because chemical analysis tends to be destructive, the first SRM's were pure chemicals, solutions, or mixtures which were carefully prepared, characterized by a standards institution and made available to users to check their measurement algorithm. The system was later refined to reduce the model ambiguity by making the relevant properties of the SRM as close to those of the object of interest as possible, giving rise to such SRM as urban dust.

A newer version of the strategy is the Standard Reference Artifact; this was initially used at NBS for neutral photographic density. These artifacts are only marginally non-ephemeral, and it was introduced to alleviate the problem. In another case, linewidth standards, it is an attempt to realize some economies of scale and provide quicker response than calibration. The problem of model ambiguities must be considered carefully since the SRA's can sometimes be of higher quality than the working standards for which they substitute. This factor is one which has always limited the effectiveness of "round robins" which depend on artifacts similar in nature to SRA's.

The most highly developed QC mechanisms for measurements are Measurement Assurance Programs. These programs, based on the pioneering collaborative work of P. Pontius and J. M. Cameron [11] at NBS in the 1960's, have become central to the Bureau's measurement services. It is difficult to explain in a few words what constitutes a MAP. A MAP is basically a measurement system which explicitly, self consciously, deliberately builds in and documents at every step tests for the properness of the measurements. MAP's are characterized by carefully thought-out redundancy and often use "self calibrating" measurement algorithms; they tend to make use of modern statistical methods and focus on the measurement results rather than on "standards" or calibrations. Hence they are software rather than hardware oriented. Since they were first applied to systems where either the quality requirements are very stringent or where the degree of assurance needed is very high, as in the accounting for Special Nuclear Materials, they are often thought of as complex and expensive to implement. This is a misconception; for a given quality or degree of assurance, they have proven to be the most efficient institution yet designed. If they have a disadvantage it is that they increase the burden on the standards organization responsible for them. This fact arises because properness must be assured on a continuing basis, and there must be a constant interchange of data and periodic exchange of artifacts between the standards lab and the operating partners. Depending on the stability of the test objects exchanged, the frequency of such exchanges may approach or equal calibration intervals. In some cases this burden can be reduced by using test objects which are more stable or rugged than the accepted standard. Voltage is such a case, where banks of fragile standard cells are compared by measurements on zener diodes.

[13] Stable is used in the expanded sense that the mean is constant during a "within group" interval; slow, well-behaved, constant changes as in the case of the slow phase change of the steel in a gage block or the slow decay of intensity of a incandescent lamp present no problems in that the mean is predictable, if not absolutely constant.

The problem of standard laboratory workload can be completely circumvented by making the standards laboratory a participant rather than an organizer. This pattern is already working for electrical quantities among the aerospace industry of the West Coast, and the Bureau has plans to formally institutionalize these regional MAP's in the future.

6. Scientific Metrology

When the measurements with which one is concerned are undertaken with a view towards understanding the physical universe, a series of issues is raised which do not exist in either technical or legal metrology.

The most important of these new issues is that the freedom to choose a measurement system on the grounds of convenience or economy is no longer legitimate. Of all the possible measurable quantities called mass or length which, in the Carnap view, are defined by the measurement system and which are logically independent and wholly arbitrary, only one can reflect the *concept* of mass which satisfies both the laws of Newton and of Einstein. The laws of physics appear to require what the wise metrologist avoids: a "true," "absolute," or *proper* quantity. A proper quantity cannot be defined by an international body, and indeed the BIPM committee on units has been careful to avoid this pitfall. A proper quantity is somehow defined by the underlying logic of the physical universe as reflected and (imperfectly) translated by the laws of physics.

The problem is to determine which quantity defined by a measurement system is the proper one. This problem has been addressed by a number of authors since it is implicit in the fundamentals of the philosophy of physics.[14] The problem could be attacked experimentally by use of a redundant set of fundamental constants.

There would have to be generated several sets of fundamental constants derived from experiments differing only in manner by which one quantity, say mass, was operationally defined by a set of measurement axioms. The self consistency of each set would then be a measure of the properness of the corresponding quantity called mass. This procedure would have to be repeated for each of the SI base quantities. It would be a monumental task, and so far has not been attempted.

There are other differences between the viewpoints of scientific and technical metrology. Experimental physics is concerned with differences between the model and object, i.e., the "name of the game" is find the model ambiguity. Except in so-called "absolute" measurements which are few and far between, any unit errors are ignored. Since the laws of physics are invariant under such errors this is understandable and explains, incidentally, why absolute determinations are so much more difficult. The physicist's attitude toward algorithm error is complicated. In an ideal experiment the experimental design would be such that the algorithm error is reduced to insignificance by including it in the model being tested. In practice, this ideal is approached in 4π radiation counting and in such experiments as Faller's [12] falling reflector "g" experiment where two SI definitions are combined in a conceptually simple measurement algorithm. Far more frequently, with more or less intellectual arrogance, it is assumed that the algorithm, or a vital part of it, is so complete that the response of the instrument can be calculated beyond the desired precision with negligible risk. This is the assumption that is not shared by the technical metrologist. Why can physicists usually get away with it? I believe there are three major reasons.

First and foremost, the assumption is often justified; as a rule, a great deal more study and design effort goes into a physics experiment than into the design of the usual metrological instrument and the physicist is unencumbered by questions of cost, manufacturing ease, reliability, and difficulty of operation. Under these conditions almost perfect algorithms can be conjured up. For example, an electron spectrograph is a horribly complex algorithm for measuring the kinetic energy of an electron, yet in an electrostatic machine the energy loss scale depends rigorously on the fact that electron energy depends on a potential function, and hence is set by its end points independent of the path connecting them. Second, generally speaking, the models (of atomic and molecular systems, for example) are very crude and the model ambiguities large, tending to "swamp" reasonable algorithm errors by their magnitude. It is notable that in the study of atomic properties "absolute" measurements and the use of internal calibration standards are much more popular than in solid state experiments where the models are even more crude. Third, for most experiments only a very few measurement algorithms exist, and only a few (usually one or two) stations exist, usually very similar. For example, the situation in electron scattering is typical where inelastic cross sections are the almost exclusive preserve of two or three university teams. Hence, almost by definition we remove the algorithm error by making the algorithm the standard in the metrological sense. Furthermore, in physics the algorithm errors tend to be of the unit variety and hence not vital to the questions of concern.

If there are realizations of the unit and the scale by an object whose model is so good that it is almost a prototype, and these realizations are easy to reproduce, it is sometimes possible to relieve the conditions on the algorithm so that temporal stability need not be proved (stability need not

[14] All previously quoted authors have addressed this problem; the best summary is Byerly and Lazara, op. cit.

even exist). A widespread example of this occurs in spectroscopy where the wavelength scale is provided by an iron arc spectrum obtained simultaneously with that of the object material. Note the very high practical virtue of such a system: one need only a satisfactory model (theory) of the object which serves as unit and scale. An object is usually the simpler of the object-instrument pair. With such an object in hand, any measurement algorithm (subject only to the restriction of being in statistical control) is valid. Any number of ordering operators can be employed and none of them need be studied in great detail nor completely understood.

Cases arise where the instrument algorithm is simpler or more convenient than the model. In this case, the unit is often attached to the algorithm and the roles of the instrument and object are inverted. Ionizing radiation measured in Roentgens is one well-known example where international comparisons involve the exchange of free air ionization chambers, i.e., detectors, not sources. Photometry is moving in this direction.

An interesting case study on the interface of scientific and technical metrology is in the measurement of luminous intensity.

The unit in this case was fixed by the International Organization as the candela, defined as the luminous intensity of 1 sq cm of a perfect radiator at the freezing point of platinum. Because of the rather peculiar nature of the unit, no choice exists (at this time) but to take as the model a perfect *hohlraum* at the freezing point of platinum and attempt to produce a test object as near to this as possible. This was done at NBS by adopting the 1932 platinum "black body" and then making a second stage model in the form of a computer code (based on earlier Canadian work). This second stage model contains all the parameters in the "black body" which are known to effect its deviation from a perfect *hohlraum*. The *hohlraum* theory can properly be considered sufficiently complete for the purpose at hand, but neither the computer model nor the knowledge of the material properties of the "black body" can so be considered. The output of the computer then contains the deviation from *hohlraum* and an idea of the ambiguities introduced by uncertainties in the material properties. No information is available as to the ambiguity introduced by approximation in the computer model, round off errors, etc.

The total ambiguity hence must be measured. Since the object in this case is the unit standard, it is impossible to determine the ambiguity since no hierarchically higher standard exists. Thus the model was used to calculate the temperature differential along the walls for which a tested algorithm exists and the deviation of this measured temperature deferential from that calculated is used as a measure of the model ambiguity. There remains the problem of quantifying the process, i.e., deriving the ambiguity in the value of luminous flux from the measurement of the ambiguity in wall temperatures.

Once the degree of model ambiguity is determined, attention must turn to assuring that the algorithm error was less than the uncertainty engendered by the model ambiguity. In this particular case the algorithm error was not known and a program was initiated to determine it. When it is determined to be less than the model ambiguity, the measurement will be made.

Note that, in this case, where the unit is frozen into the politics of the SI system, at some point one must either accept the total uncertainty implied by the irreducible model ambiguity or attack the political problem of disengaging the unit from this model and attaching it to a model of lower inherent ambiguity. In fact such a political solution has been achieved.

7. Summary

There exists a reasonably complete and coherent body of theory concerning the fundamentals of metrology. It is considerably more complex than has been expounded here, but a thoughtful application of the principles dealt with will avoid many of the problems which arise in on-going measurement systems in the field of technical or legal metrology.

This document had its origin in lecture notes for the course given by George Washington University Department of Continuing Education on Calibration Laboratory Management which I have taught for several years, and a series of seminars given over the past decade at the National Bureau of Standards. Many of the principles expounded have been developed or articulated in collaboration with Paul Pontius, Joe Cameron, Churchill Eisenhart, Chester Page, and others at NBS whose contributions to my education I can never sufficiently acknowledge.

8. References

[1] Ellis, Brian. *Basic concepts of measurement.* Cambridge: Cambridge University Press; 1966. 219 p.

[2] Eisenhart, Churchhill. Realistic evaluation of precision and accuracy of instrument calibration systems. J. Res. Nat. Bur. Stand. (U.S.). 67C(2); 161-187; 1963 April-June. This and other fundamental papers can be found in Precision Measurement and Calibration, NBS Spec. Publ. 300, Vol. 1 (1969 February).

[3] Volodreskii, Effect on precision of measurements of the discrepancy between the investigated object and its model, (translated from Izmeritel 'naya Technika, No. 7, pp. 18-20, July 1969) Measurement Techniques No. 7, p. 907 (1969).

[4] Carnap, Rudolph. *Philosophical foundations of physics.* New York: Basic Books; 1956. 300 p.

[5] Pontius, Paul, Mass measurement: A study of anomalies science. **190** (4212): 379-380; 1974 October.

[6] Schoonover, R. M.; Davis, R. S.; Driver, R. G.; Bower, V. E. A practical test of the air density equation in standards laboratories at differing altitudes. J. Res. Nat. Bur. Stand. (U.S.) **85** (1): 27-38, 1980 January-February.

[7] Bridgeman, Percy W. *Logic of modern physics.* New York: Macmillan Co.; (1927) 228 p.

[8] Byerly, H. C.; Lazara, V. A. Realistic foundations of measurement. philosophy of science. **40** (1): 10-28; 1973 March.

[9] Whitehead, T. N. *The design and use of instruments and accurate mechanism.* New York: Macmillan Co.; 1934. 283 p.

[10] Belanger, Brian C. Traceability: An evolving concept. ASTM Standardization News. **8** (1): 22-28; 1980 January.

[11] Pontius, P. Measurement philosophy of the pilot program for mass calibration. Nat. Bur. Stand. (U.S.) Tech Note 288; 1966 May. 39 p.

Pontius, P. E.; Cameron, J. M. Realistic uncertainties and the mass measurement process. Nat. Bur. Stand. (U.S.) Monogr. 103; 1967 August. 20 p. (Republished with new figure placement in NBS Spec. Publ. 300, Vol. **1**, 1969 February).

[12] Faller, J. E. Precision measurement of the acceleration of gravity. science. **158** (3797): 60-67; 1967 October 6.

JOURNAL OF RESEARCH of the National Bureau of Standards
Vol. 86, No. 3, May-June 1981

Absolute Determination of the Thermal Conductivity of Argon at Room Temperature and Pressures Up to 68 MPa

C.A.N. deCastro* and H.M. Roder**

National Bureau of Standards, Boulder, CO 80303

January 5, 1981

The thermal conductivity of argon at room temperature and for pressures up to 68 MPa has been measured with a transient hot-wire technique in order to assess the accuracy of an instrument of this type. The data are presented for a nominal temperature of 300.65 K and comparison with other authors shows that our data is accurate to within ± 1 percent, and it is the most accurate set of data for pressures above 35 MPa. Experimental evidence of a thermal conductivity enhancement near the critical density for a temperature about twice the critical temperature is herein reported. The experimental data were compared with the values predicted by the hard sphere model and it has been found that the theory gives values that are about 4 percent lower than the experimental ones in the density range 0–400 kg/m³ and about 1 to 2 percent lower in the high density region 400–825 kg/m³.

Key words: Ambient temperature; argon; critical enhancement; hard sphere; hot wire; thermal conductivity; transient

1. Introduction

Thermal conductivity of fluids has proved to be one of the most difficult transport properties to measure with a high accuracy, and only during the last decade has the development of the transient hot wire technique both for the gaseous phase [1–3][1] and liquid phase [4–6] made possible an accuracy of ± 0.3 percent for gases and ± 0.6 percent for liquids.

A new apparatus of the transient hot wire technique has been developed [7] to measure the thermal conductivity of fluids in the temperature range 70–320 K with pressure to 70 MPa. We report here the measurements obtained for argon at 300.65 K.

The purpose of this work is twofold: to assess the accuracy of the present instrument and to extend the pressure range of the high accuracy data obtained by Kestin, et. al. [2] at the same temperature. The extrapolation of our data to zero density coupled with the zero density viscosity obtained from the work of Kestin, et. al. [8] yields a value of the Eucken factor.

$$Eu = \frac{4\lambda_o M}{15 R \eta_o} \frac{f_\eta}{f_\lambda} = 1.0029 \qquad (1)$$

This in principle could support an uncertainty of not more than 0.3 percent. However, the precision of the experimental points is ± 0.6 percent when averaged over all densities and that suggests an overall accuracy of the data no better than ± 1.0 percent.

When we attempted to correlate the data with a low order polynominal

$$\lambda = \lambda_o + a_1 \varrho + a_2 \varrho^2 \qquad (2)$$

we obtained an S-shaped deviation plot which was clearly non-random. A detailed examination of the experimental data in the density range 5 to 15 mol/L (200 kg/m³ to 700 kg/m³) shows an anomalous increase in the thermal conductivity of up to 0.6 mW/m•K, which we attribute to a critical point enhancement even though the temperature is about twice the critical temperature.

To explore this unexpected behavior further we have applied the hard sphere model to the interpretation of the thermal conductivity of argon [9–11]. The difference between the experimental values and the calculated ones supports the existence of a critical point enhancement, as the hard sphere model agrees with the experimental values to within 0.7 mW/m•K or about 3.5 percent at densities below 5 mol/L and about 1.5 percent at densities above 15 mol/L. However, for densities between 5 and 15 mol/L where we find a critical enhancement the deviations run up to 1.35 mW/m•K, or about 5 percent. However, the magnitude of

*Centro de Quimica Estrutural, Instituto Superior Technico, 1096 Lisboa Codex, PORTUGAL

**Center for Chemical Engineering, National Engineering Laboratory

[1]Figures in brackets indicate literature references at the end of this paper.

the enhancement when established from a curve fit to the data is about 2.5 percent. Dymond [10], in an extension of the hard sphere model to dilute gases, found that for temperatures up to 1.7 T_c the thermal conductivities of argon determined by Michels, et al. [12] and Le Neindre, et al. [13] showed a similar critical enhancement, larger than the one reported here because of the lower temperatures involved. Dymond concluded that the hard sphere model is unable to account for the anomalous behavior of the thermal conductivity data.

2. The Principle of Operation

A detailed description of the hot-wire instrument will be given in a separate paper [7]; however, some of the more important details are given here.

For the transient hot-wire technique, a thin platinum wire immersed in the fluid and initially in thermal equilibrium with it, is subjected at time $t = 0$ to a step voltage applied to it. The wire will behave as a line source of heat with constant magnitude q.

The physical arrangement closely models an ideal line source, and the transient heat conduction equation, the temperature increase in the wire, ΔT is given by

$$\Delta T = \frac{q}{4\pi\lambda(T_r, \varrho_r)} \ell n \left(\frac{4K_o}{a^2 C} t\right) \tag{3}$$

where

$$T_r = T_o + \tfrac{1}{2}[\Delta T(t_1) + \Delta T(t_2)] \tag{4}$$

and

$$\Delta T = \Delta T_w - \Sigma\, \delta T_i \tag{5}$$

$K_o = \lambda(T_o, \varrho_o)/\varrho_o\, Cp_o$ is the thermal diffusivity of the fluid at the bath temperature when $t = 0$; a is the radius of the wire; and $\ell n\, C = \gamma$, where γ is Euler's constant. The times t_1 and t_2 are the initial and final times of measurement, and ΔT_w is the experimentally determined temperature rise in the wire. The corrections δT_i have been fully described elsewhere [1] and they account for the departure of the real instrument from the ideal model. Of these corrections the most important at lower times is δT_1, the effect of the finite heat capacity of the wire.

3. Description of the Instrument

Figure 1 shows the circuitry employed. Use of a Wheatstone bridge provides end effect compensation and follows the general development of the hot wire instrument pioneered by Haarman [14], de Groot, et al. [15], and Castro, et al. [16]. However, instead of measuring values of time corresponding to a bridge null with a fixed set of predetermined resistors, in the present instrument the voltage developed across the bridge is measured directly as a function of time with a fast response digital voltmeter (DVM). The DVM is controlled by a minicomputer which also handles the switching of the power and the logging of the data. The automation of the voltage measurement follows the work of Mani [17] who used a similar arrangement with a transient hot wire cell to measure resistance by the four lead technique rather than using a bridge.

Each arm of the bridge is designed to be 100 Ω, two arms R_1 and R_2 are standard resistors. The resistance in each of the other arms is a composite of the hot wire, leads into the cryostat and a ballast resistor. The ballast resistors allow each working arm to be adjusted to a value of 100 Ω.

The measurement of thermal conductivity for a single point is accomplished in two phases. In the first phase the bridge is balanced as close to null as is practical. With a very small applied voltage, 0.1 v normally, i.e., essentially at bath or cell temperature, the lead resistances are read on channels 1 and 7, the hot wire resistances on channels 3 and 4, and the ballast resistors on channels 2 and 5. For these measurements switch 1 is turned from dummy to the bridge while switch 2 is open. The ballasts are adjusted until each leg is approximately 100 Ω. Finally, with switch 2 closed, the bridge balance is checked on channel 6. The second phase incorporates the actual thermal conductivity measurement. The power supply is set to the applied power desired, switch 2 is closed, and switch 1 switched from dummy to bridge. The voltage developed across the bridge as a function of time is read on channel 6 and stored. The basic data is a set of 250 readings taken at 3 ms interval. Finally the voltage on channel 0 is read to determine the exact applied power. The cell temperature is found using a standard [18] arrangement of platinum resistance thermometer and six dial microvolt potentiometer. The pressure in the cell is read from a calibrated spiral steel bourdon tube using an associated optical read out. All of the pertinent data is written by the minicomputer onto a magnetic tape for subsequent evaluation. The cryostat, filling system, temperature controllers are described elsewhere [7].

An experimental run is a collection of individual points, usually an isotherm. For each run the data on the magnetic tape is processed point by point on a large computer. In addition to the reduction of the raw data, i.e., the conversion of bridge offset voltages to resistance changes and then to temperature changes of the wire, the set of 250 temperature changes is plotted as ΔT vs. $\ell n(t)$ for every point. The computer also evaluates the best straight line for the ΔT-$\ell n(t)$ data and determines the thermal conductivity $\lambda(T_r, \varrho_r)$ from the slope of this straight line. A second plot for every thermal conductivity point shows the "scattering

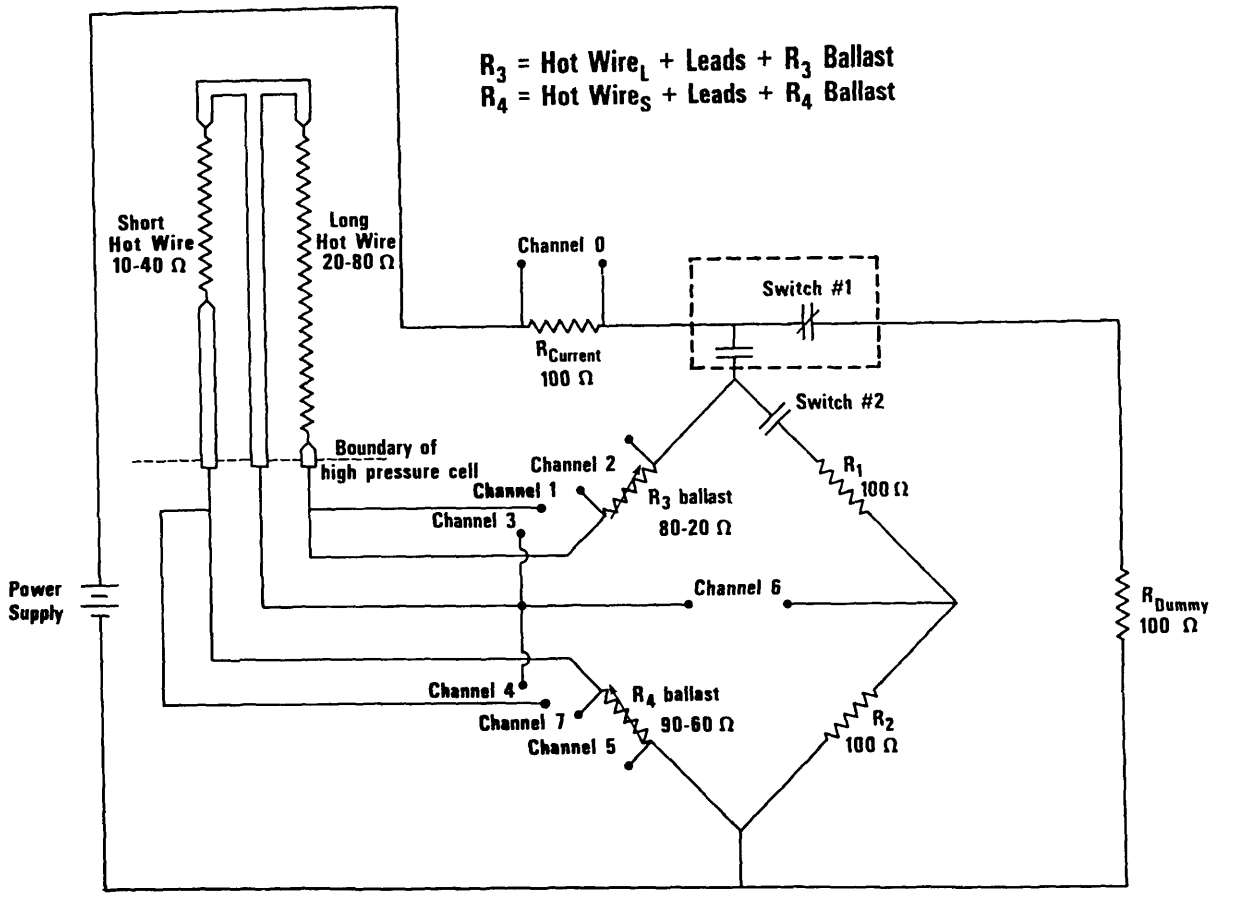

FIGURE 1. Circuit diagram of the hot wire apparatus.

diagram," i.e., the deviations of the set of 250 temperature changes from the calculated straight line.

4. Wire Calibration

In order to obtain the temperature increase of the platinum wires from the corresponding resistance increase, we need to know the variation of resistance with temperature for both wires. It has been shown in the past [4, 16, 19, 20] that an in situ calibration of the wires is desirable and also that the resistances per unit length of both wires must not differ by more than 2 percent. In addition, if they differ by more than 0.3 percent a correction to the temperature increase of the wire and to the heat generated in the long wire, functions of the resistances per unit length in both wires, must be applied [20].

The wire resistances measured at essentially zero applied power in the balancing of the bridge together with the cell temperatures as determined from the platinum resistance thermometer are taken as the in situ calibration of the wires. Some 1500 values were collected for each wire in the temperature range 150-320 K with pressures from atmospheric to about 70 MPa. The resistance relation for each wire is represented by an analytical function of the type

$$R(T) = A + B \cdot T + C \cdot T^2 + D \cdot P \qquad (6)$$

where T is the temperature in kelvin and P the gage reading. The pressure dependence is small but statistically significant and reflects the fact that the calibration measurements are made with a small applied power of 0.1 v. The constants obtained are presented in table 1. The long wire has a length of 10.453 cm at room temperature, the short wire one of 5.143 cm. Both wires have a nominal diameter of 0.00127 cm, thus the radius a in eq (3) is 0.000625 cm. Knowing that the length of both wires is a function of temperature, we can evaluate

$$\sigma_L = \frac{R_L(T)}{\ell_L(T)} \text{ and } \sigma_S = \frac{R_S(T)}{\ell_S(T)} \qquad (7)$$

and compare σ_L and σ_S in the experimental temperature range. Figure 2 shows the percent difference between σ_L and σ_S as a function of T and it can easily be seen that this

TABLE 1. *Calibration Constants of Wires*

	A/Ω	B/ΩK^{-1}	C/ΩK^{-2}	D/Ω (MPa)$^{-1}$	σ_0^*/Ωm^{-1}
Long wire	−9.065472	0.3534445	$-0.5923443 \times 10^{-4}$	-1.40146×10^{-3}	794.7
Short wire	−4.346459	0.1740251	$-0.2831553 \times 10^{-4}$	-6.56582×10^{-4}	798.8

σ_0^* is the resistance per unit length of each wire at 0.1 MPa and 273.15 K.

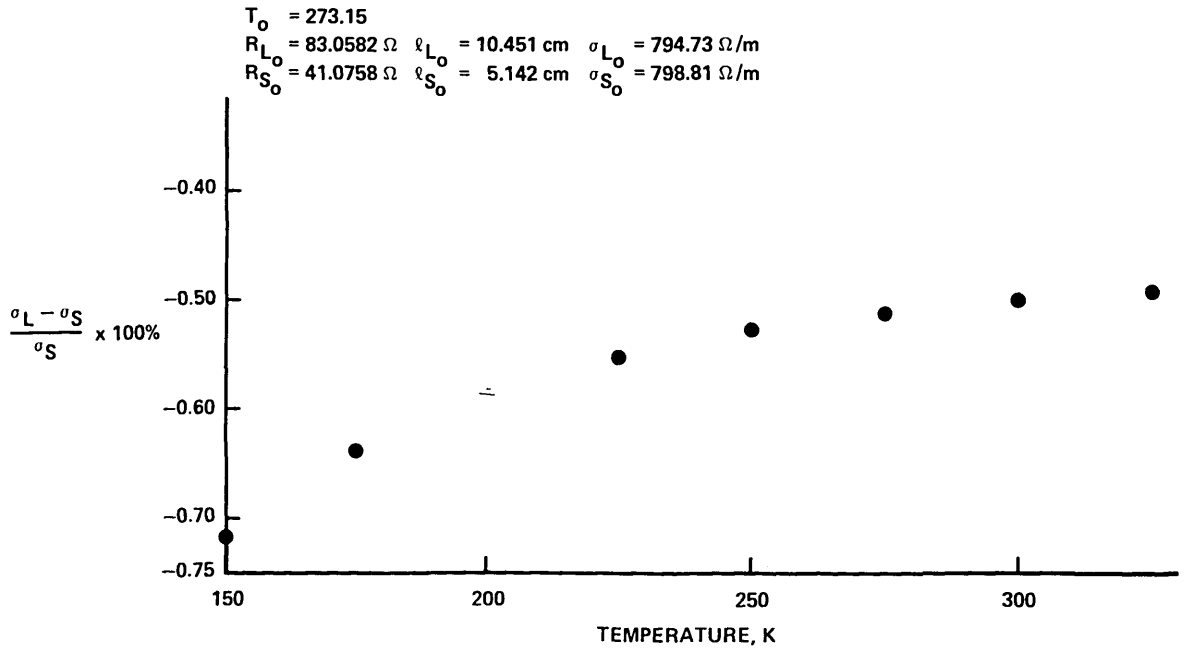

FIGURE 2. Wire calibration, resistance per unit length vs. temperature.

departure is no greater than 0.5 percent. The departure in figure 2 is as might be expected because the wires in the instrument were purposely left in the unannealed state. We are, therefore, justified in ignoring the correction proposed by Kestin and Wakeham [20].

5. Experimental Procedure

The wires and their supports are enclosed in a pressure vessel [7] which is operated at a nominal temperature of 296.1 K and controlled to within ± 0.002 K. The cell is filled with argon, maximum imprity 347 ppm, mostly oxygen. The gas was then compressed to about 70 MPa and allowed to cool to cell temperature before any measurements were taken. A series of measurements at different applied powers was made at a given level of pressure and then a small nearly isochoric expansion was made. The gas was allowed to warm up and reach equilibrium, then a new set of measurements at the new pressure level was taken. The applied power was varied in such a way that the total temperature increase in the wires ranged between 1 and 5 K. The time interval of measurement in the instrument can be varied, however we held the interval of measurement to 3 ms and the duration of the measurement to 0.75 s in order to avoid the onset of natural convection. The density of argon was taken from the equation of state developed at NBS [21, 22].

The total number of points taken was 112, with an average of four different power levels at each level of density or pressure. Overlap of density range in different working days was done to assess the longer term reproducibility of the instrument.

6. Performance of the Instrument

The analysis of the theory of the transient hot wire indicates that the corrected temperature rises of the wire ΔT must be a linear function of $\ell n(t)$ over the range of experimental measurements, provided that the instrument conforms to the ideal mathematical model.

Figure 3 shows the corrected temperature rises of the wires as a function of $\ell n(t)$, including the straight line fitted for a typical experimental point, 29062, in argon at the equilibrium temperature T_o = 300.168 K, and pressure, P = 18.879 MPa. Although the data set starts at 0.003 s, the plot begins at 0.033 s. In addition, it was found that the correction δT_1 was only of the order of 1 percent of ΔT for times around 0.15 s. At present no reliable correction δT_1 valid for $\delta T_1 > 1$ percent of ΔT is available. Therefore, the least squares straight line fitting considered only that part of the data set between times of 0.154 s and 0.755 s. Of the total of 250 individual measurements 200 are used in the fitting, the first 50 measurements are neglected. The onset of convection is determined as a deviation from the straight line at long times. Several trial runs established that for nearly all densities this process occurs around 1 s. However, at the very lowest densities measured the onset of convection occurs at experimental times less than 0.755 s, and for these points a second variable portion of the data set at long times had to be omitted from the least squares analysis.

Figure 4 shows the companion plot for point 29062, the deviations of the corrected temperature rises of the wires from the straight line fitting for that part of the data set between times of 0.033 s and 0.755 s. It is evident that for times valid in the least squares fitting, namely 0.154 s to 0.755 s, that data set departs by less than 0.8 percent from the regression line and that there is no evidence of a systematic curvature. A statistical evaluation of the error band for the slope of the least squares straight line is included in the output from the data reduction program.

To obtain the thermal conductivity from the slope we must use the value of q, the heat dissipation per unit length, which was found to be constant to within ± 0.1 percent during the measuring time.

The reproducibility of the instrument is obtained through an intercomparison of experimental points at the same nominal temperature and the same nominal density taken for different heat inputs. Table 2 shows one such set of experimental points obtained on two different days with different fillings at a density near 2.9 mol/L (116 kg/m³). The

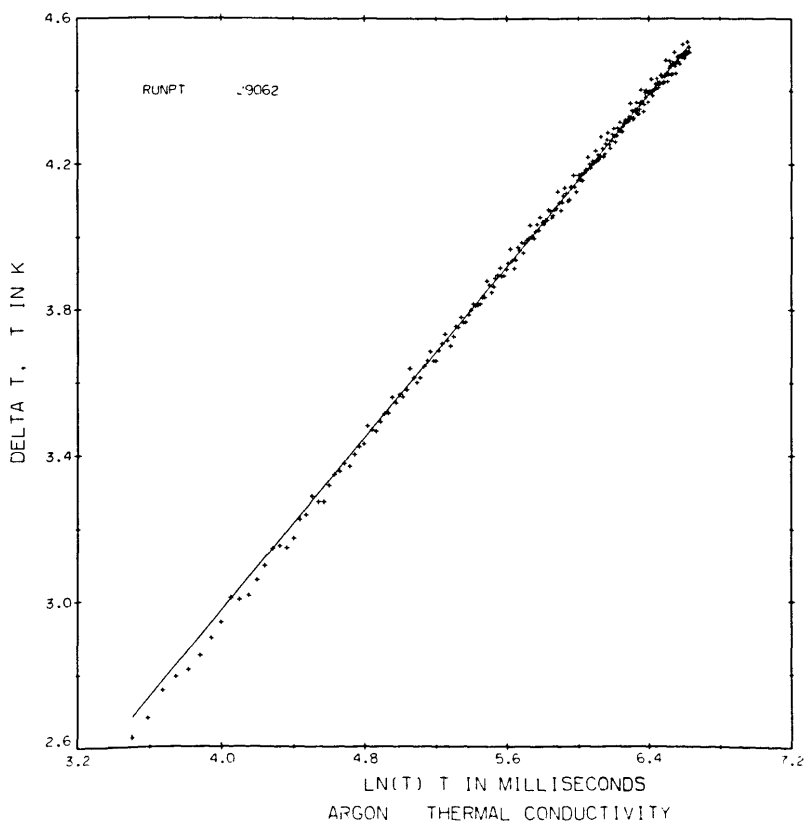

FIGURE 3. Typical rises in wire temperature vs. logarithm of time.

experimental thermal conductivities are adjusted a nominal temperature of $T_{nom} = 300.65$ K for the small temperature difference $T - T_{nom}$, following the argument that the excess thermal conductivity $\lambda(\varrho, T) - \lambda_0(0, T)$ is a function of density alone [2]. Hence

$$\lambda(T_{nom}, \varrho_r) = \lambda(T_r, \varrho_r) + \left(\frac{\partial \lambda}{\partial T}\right)_{\varrho, T_{nom}} (T_{nom} - T_r) \tag{8}$$

with

$$\left(\frac{\partial \lambda}{\partial T}\right)_{\varrho, T_{nom}} = \left(\frac{\partial \lambda_0}{\partial T}\right)_{T_{nom}} = 0.0501 \text{ mW/m•K}^2 \tag{9}$$

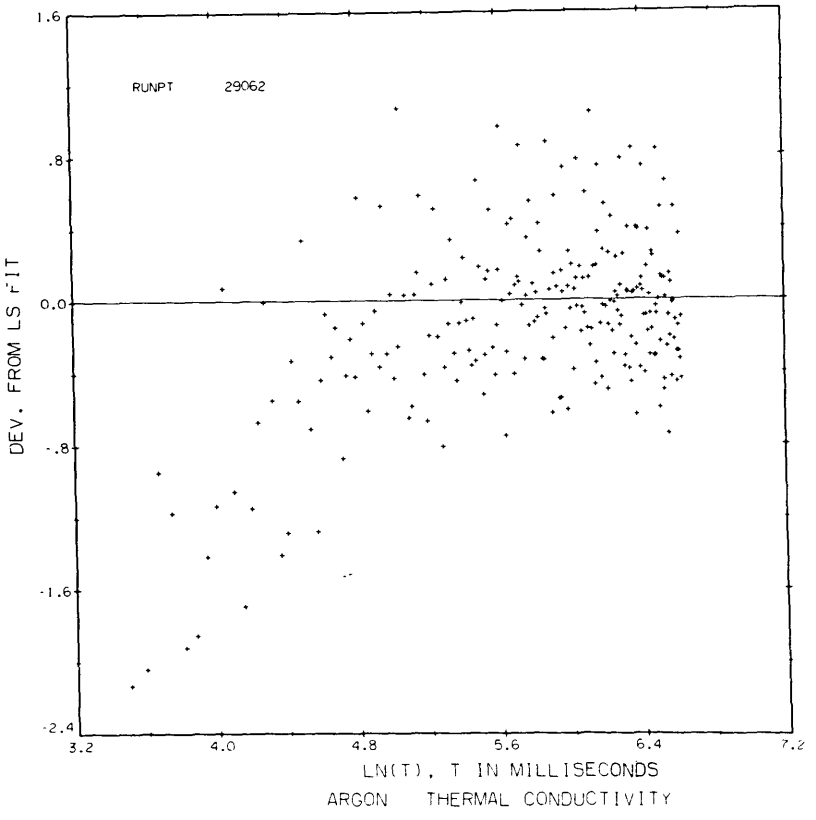

FIGURE 4. Typical deviations of the rise in wire temperature from the best straight line vs. logarithm of time.

TABLE 2. *Test of Reproducibility*

T_{nom} = 300.65 K ϱ_{nom} = 2.9 mol/L (116 kg/m³)

Run Pt	Pressure	T_r	Density	Thermal Conductivity W/m•K		
	MPa	K	mol/L	$\lambda(T_r, \varrho)$	$\lambda(T_{nom}, \varrho)$	$\lambda(T_{nom}, \varrho_{nom})$
29077	6.923	300.385	2.8572	.02044	.02045	.02049
29107	6.981	301.371	2.8706	.02054	.02050	.02052
29076	6.926	298.775	2.8772	.02034	.02043	.02045
29106	6.981	300.462	2.8812	.02041	.02042	.02043
29075	6.927	297.597	2.8914	.01997	.02012	.02013
29105	6.983	298.784	2.9015	.02024	.02033	.02033
29104	6.983	298.148	2.9090	.02024	.02037	.02036
29103	6.984	297.609	2.9161	.02026	.02041	.02040
						0.02039 ± 0.00012

The points are then further adjusted to an even density of 2.9 mol/L using a value of $(\frac{\partial\lambda}{\partial\varrho})T_{nom}$, ϱ_{nom} = 0.001 W•L/m•K•mol as shown in the last column of table 2. The average value for the eight points at T_{nom} = 300.65 K and ϱ_{nom} = 2.9 mol/L is 0.02039 ± 0.00012 W/m•K, the variance of this sample being ± 0.6 percent. The variance was found to be roughly the same for all densities, thus the precision of the instrument is on the order of ± 0.6 percent.

The accuracy of the instrument could be obtained from the value of the Eucken factor, equation (1), and the value obtained, 1.0029, through the extrapolated value of $\lambda(0, T_{nom})$ in a low density fitting of $\lambda(\varrho)$. However, considering the reproducibility to be ± 0.6 percent, and considering that the deviation of a set of ΔT data from its regression straight line is quite often closer to 0.8 percent, we shall regard the 0.3 percent obtained in the low density extrapolation as a fortunate coincidence, and claim an overall accuracy of ± 1 percent for the values of thermal conductivity.

7. Results and Analysis of the Data

Table 3 presents the 112 points obtained for argon in the density range 0.6 to 20 mol/L (24 to 820 kg/m³). The last column in table 3 shows the value of thermal conductivity adjusted to a nominal temperature of 300.65 K. Figure 5 shows the experimental values for the thermal conductivity of argon in the full density range and compares it with values by Kestin, et al. [2] (0-530 kg/m³), values by Michels, et al. [12] and values by Le Neindre, et al. [13]. The four sets of data agree within their mutual uncertainties of ± 1.0 percent, ± 0.3 percent, ± 2 percent and ± 3 percent respectively. Following the well known density dependence of thermal conductivity for moderately dense gases we tried to fit a curve of the type

$$\lambda = a_o + a_1\varrho + a_2\varrho^2 \qquad (10)$$

which is often used in place of the more rigorous expression, to our data. Initially we used the entire set of data, i.e., all densities up to 20 mol/L. Figure 6 shows the departure plot for this fit. Considering our precision to be ± 0.6 percent the S-shaped deviation shown in figure 6 is clearly nonrandom. This in turn implies that the functional form of the fitting function equation (10) is not appropriate. What is clear from this departure plot is that in order to get a valid extrapolation to zero density with a low order polynominal

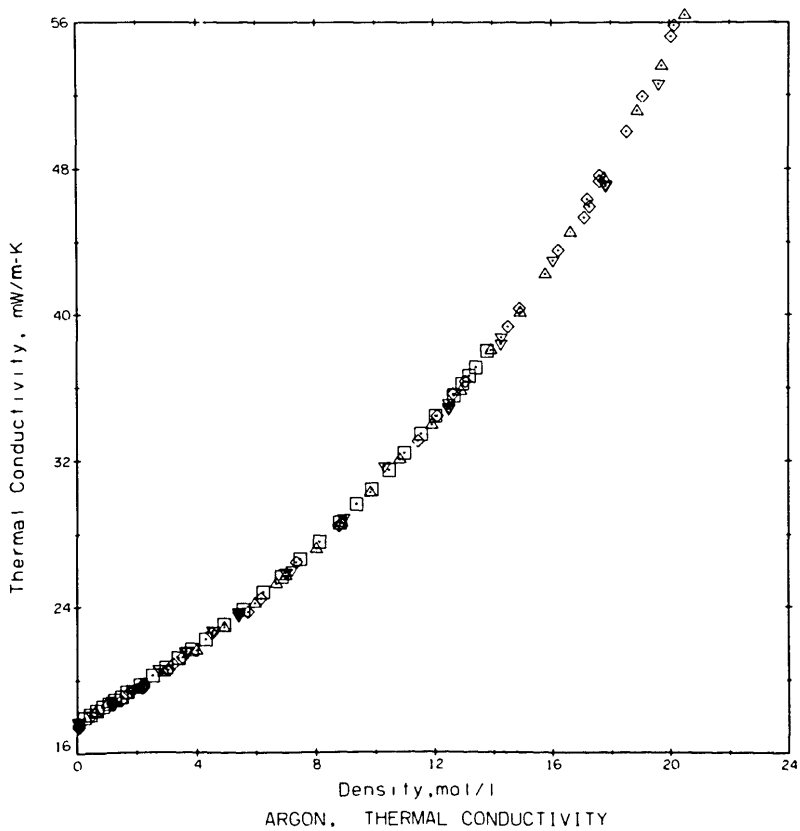

FIGURE 5. Thermal conductivity of argon at 300.65 K vs. density. △ this paper, ⊡ Kestin, et al. [2], ⊡ LeNeindre, et al. [13], ▽ Michels, et al. [12].

TABLE 3. *Experimental thermal conductivity values for argon.*

Run Pt	Press MPa	Temp K	Dens mol/L	Power W/m	ThermC W/m•K	Stat*	TC300.65 W/m•K
29123	1.461	304.195	.5811	.20246	.01835	.013	.01817
29122	1.462	301.738	.5863	.14149	.01830	.021	.01825
29121	1.462	299.669	.5905	.09143	.01804	.035	.01809
29120	1.462	298.025	.5939	.05225	.01832	.082	.01845
29084	2.412	300.384	.9759	.11518	.01869	.013	.01870
29083	2.413	299.468	.9794	.09146	.01868	.019	.01874
29082	2.413	298.709	.9824	.07048	.01874	.028	.01884
29081	2.414	297.883	.9856	.05227	.01839	.042	.01853
29119	2.996	309.226	1.1776	.35692	.01928	.004	.01885
29118	2.996	306.236	1.1904	.27420	.01906	.004	.01878
29117	2.996	303.507	1.2020	.20237	.01892	.007	.01878
29116	2.996	301.104	1.2125	.14150	.01879	.008	.01877
29115	2.996	299.370	1.2201	.09139	.01872	.027	.01878
29114	2.996	297.808	1.2271	.05224	.01841	.059	.01855
29080	4.758	299.859	1.9497	.11515	.01948	.014	.01952
29113	4.892	307.669	1.9476	.35706	.01964	.006	.01929
29079	4.759	299.059	1.9560	.09145	.01905	.019	.01913
29112	4.892	305.395	1.9642	.27417	.01989	.005	.01965
29078	4.760	297.714	1.9664	.05225	.01911	.043	.01926
29111	4.892	302.903	1.9827	.20239	.01968	.006	.01957
29110	4.892	300.779	1.9988	.14145	.01957	.010	.01956
29109	4.893	299.028	2.0126	.09141	.01936	.019	.01944
29108	4.893	297.710	2.0229	.05224	.01925	.043	.01940
29077	6.923	300.385	2.8572	.14146	.02044	.010	.02045
29107	6.981	301.371	2.8706	.17056	.02054	.008	.02050
29076	6.926	298.775	2.8772	.09145	.02034	.021	.02043
29106	6.981	300.462	2.8812	.14143	.02041	.009	.02042
29075	6.927	297.597	2.8914	.05225	.01997	.042	.02012
29105	6.983	298.784	2.9015	.09140	.02024	.020	.02033
29104	6.983	298.148	2.9090	.07040	.02024	.029	.02037
29103	6.984	297.609	2.9161	.05218	.02026	.045	.02041
29074	9.190	299.991	3.8313	.14153	.02137	.010	.02140
29073	9.194	298.556	3.8567	.09146	.02117	.021	.02127
29072	9.199	297.371	3.8787	.05223	.02114	.049	.02130
29102	9.686	300.836	4.0303	.17037	.02182	.008	.02181
29101	9.687	300.007	4.0450	.14130	.02177	.011	.02180
29100	9.688	298.560	4.0710	.09129	.02174	.022	.02184
29099	9.689	298.015	4.0810	.07035	.02155	.029	.02168
29071	11.609	301.155	4.8495	.20247	.02260	.009	.02257
29098	11.700	301.303	4.8851	.20215	.02298	.007	.02295
29070	11.612	299.541	4.8856	.14147	.02278	.014	.02284
29069	11.612	298.361	4.9116	.09132	.02276	.023	.02287
29097	11.701	299.745	4.9197	.14125	.02288	.012	.02293
29096	11.702	298.396	4.9499	.09129	.02270	.021	.02281
29095	13.812	301.069	5.7953	.20216	.02420	.011	.02418
29094	13.813	299.516	5.8370	.14128	.02381	.013	.02387
29068	14.183	300.847	5.9597	.20200	.02434	.008	.02433
29067	14.183	299.297	6.0025	.14120	.02418	.013	.02425
29066	14.184	298.105	6.0365	.09124	.02422	.024	.02435
29092	15.730	300.736	6.6210	.20216	.02525	.008	.02525
29089	15.732	299.969	6.6457	.17044	.02523	.009	.02526
29086	15.737	299.309	6.6687	.14132	.02531	.013	.02538
29085	15.772	299.555	6.6756	.14124	.02533	.013	.02538
29091	15.730	298.605	6.6875	.11497	.02512	.018	.02522
29087	15.734	298.011	6.7082	.09137	.02497	.025	.02510
29065	16.451	300.459	6.9344	.20198	.02572	.008	.02573
29064	16.454	299.103	6.9801	.14116	.02569	.013	.02577

TABLE 3. *Experimental thermal conductivity values for argon. (continued)*

Run Pt	Press MPa	Temp K	Dens mol/L	Power W/m	ThermC W/m·K	Stat*	TC300.65 W/m·K
29063	16.454	297.951	7.0184	.09124	.02544	.025	.02558
29062	18.879	300.168	7.9569	.20201	.02723	.008	.02725
29061	18.882	297.781	8.0498	.09124	.02694	.027	.02708
29060	21.041	301.382	8.7832	.27374	.02870	.006	.02866
29059	21.043	299.856	8.8475	.20206	.02851	.008	.02855
29058	21.044	298.723	8.8960	.14119	.02849	.015	.02859
29018	23.481	302.213	9.6941	.35561	.02983	.005	.02975
29057	23.679	300.997	9.8244	.27376	.03054	.006	.03052
29056	23.681	299.696	9.8854	.20201	.03018	.008	.03023
29055	23.682	298.414	9.9462	.14116	.03022	.016	.03033
22054	26.202	300.783	10.7689	.27371	.03205	.007	.03204
29053	26.205	299.445	10.8368	.20205	.03196	.010	.03202
29052	26.208	298.337	10.8942	.14121	.03155	.017	.03167
29014	26.498	300.188	10.9051	.27320	.03235	.006	.03237
29051	29.172	300.418	11.8240	.27533	.03427	.007	.03428
29050	29.174	299.255	11.8868	.20201	.03350	.011	.03357
29012	29.462	300.076	11.9397	.27324	.03409	.013	.03412
29049	29.177	298.195	11.9450	.14116	.03358	.018	.03370
29011	29.464	297.705	12.0688	.14100	.03390	.018	.03405
29048	32.339	300.161	12.8650	.27378	.03576	.006	.03578
29047	32.342	298.995	12.9312	.20207	.03562	.011	.03570
29046	32.342	298.097	12.9820	.14118	.03577	.018	.03590
29045	35.633	301.174	13.7911	.35636	.03803	.005	.03800
29044	35.634	299.942	13.8620	.27378	.03780	.007	.03784
29008	35.944	300.660	13.9090	.35592	.03844	.006	.03844
29004	35.943	300.636	13.9100	.35603	.03833	.005	.03833
29043	35.636	298.805	13.9281	.20213	.03780	.012	.03789
29007	35.944	299.506	13.9755	.27344	.03759	.009	.03765
29042	35.639	297.878	13.9832	.14124	.03764	.019	.03778
29003	36.014	299.434	13.9995	.27348	.03783	.008	.03789
29002	35.943	297.991	14.0633	.20171	.03830	.012	.03843
29001	35.941	297.734	14.0779	.14120	.03750	.019	.03765
29005	35.943	297.481	14.0932	.14107	.03832	.020	.03848
29041	39.399	300.710	14.8433	.35650	.04009	.006	.04009
29040	39.401	299.670	14.9047	.27378	.04012	.008	.04017
29039	39.401	298.695	14.9622	.20205	.04014	.012	.04024
29038	39.403	297.775	15.0174	.14124	.03978	.021	.03992
29036	42.981	300.625	15.7366	.35638	.04202	.006	.04202
29037	42.978	299.395	15.8087	.27389	.04225	.009	.04231
29035	42.983	298.473	15.8648	.20211	.04220	.013	.04231
29033	46.726	300.320	16.6035	.35637	.04445	.007	.04447
29034	46.723	299.253	16.6659	.27382	.04455	.009	.04462
29032	46.729	298.283	16.7252	.20204	.04430	.011	.04442
29031	52.190	300.095	17.7302	.35635	.04735	.006	.04738
29030	52.190	298.226	17.8407	.20206	.04748	.013	.04760
29029	58.578	300.830	18.8360	.44999	.05099	.004	.05098
29028	58.578	299.852	18.8926	.35636	.05117	.007	.05121
29027	58.580	298.024	19.0000	.20199	.05113	.016	.05126
29026	63.535	299.687	19.7015	.35602	.05357	.007	.05362
29025	63.538	298.024	19.7983	.20189	.05343	.016	.05356
29024	68.709	300.446	20.4228	.45004	.05638	.005	.05639
29023	68.710	299.553	20.4738	.35661	.05604	.008	.05609
29022	68.710	298.724	20.5213	.27399	.05621	.010	.05631
29021	68.709	298.014	20.5620	.20224	.05637	.017	.05650
29020	68.709	297.413	20.5966	.14140	.05642	.030	.05658

*The data reduction program determines both a value for the slope and its uncertainty, i.e., slope = S ± 2.1 σ. Printed here is STAT = 2.1 σ/S.

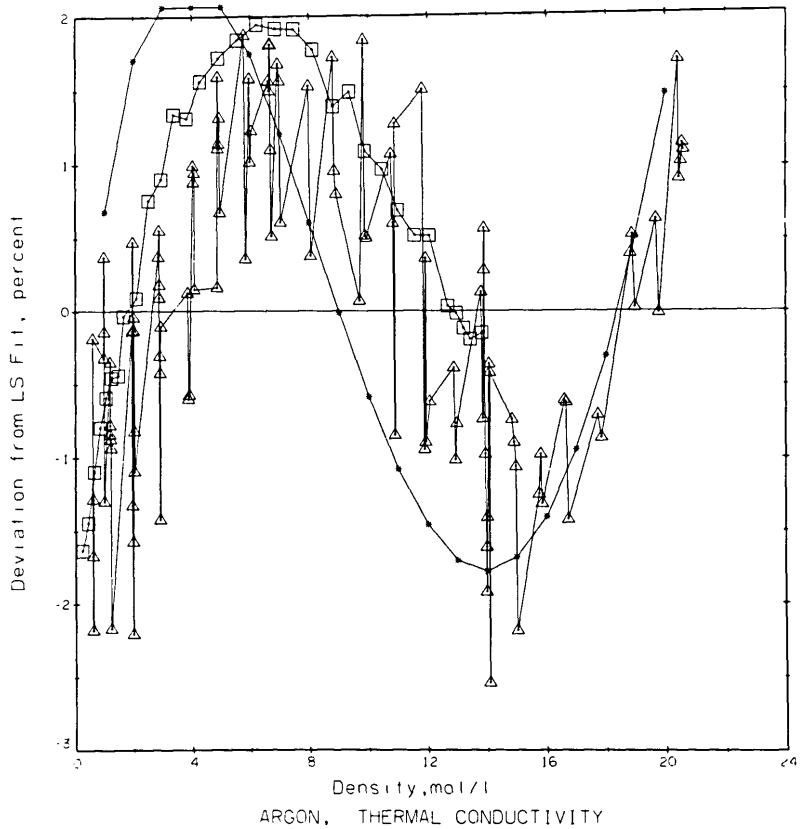

FIGURE 6. Deviations of the curve fit of equation 10 for the entire range of densities vs. density. △ this paper, ⊡ Kestin, et al. [2], * Hanley, et al. [22].

we should fit to densities no higher than about 7 mol/L, i.e., the first 56 points only of table 3. The departure plot for a fit over this reduced range in density is shown in figure 7. In this plot the departures are indeed random as the one sigma and two sigma error bands show. Table 4 shows the coefficients obtained for both density ranges including the statistical errors of the coefficients. Included for comparison in figures 6 and 7 are the experimental thermal conductivities of Kestin, et al. [2] and the values predicted by the correlation of Hanley, et al. [22]. The latter is based on the data reported by Michels, et al. [12] and Le Neindre, et al. [13].

We propose that there is an anomalous increase in the thermal conductivity which we attribute to a critical enhancement even though the temperature here T_{nom} = 300.65 K is about twice the critical temperature. To prove the existence of an enhancement we did a special curve fit to which the following considerations applied: (1) we will constrain the isotherm through the proper zero density value; (2) we will use a functional form that is appropriate, yet is also highly constrained; (3) looking at figure 6 we will fit only data between 0 and 7 mol/L as well as data above 14 mol/L in density and look at the deviation plot for densities between 7 and 14 mol/L. The equation selected has been used with some success to separate the background thermal conductivity from the critical component (see for example ref. 22).

$$\lambda = A + B\varrho + C\left\{e^{D\varrho} - 1.0\right\} \qquad (11)$$

In the fit to be described A is constrained to be 0.01783 W/m•K, D is a fixed value of 0.060 while B and C are treated as parameters to be determined. The cutoff points in density actually used are 5 and 15 mol/L and the deviation plot of this fit is shown in figure 8. The plot shows that the deviations for densities between 0 and 5 mol/L and between 15 to 20 mol/L are random, and it clearly illustrates the nature and size of the enhancement. In particular, figure 8 shows that the enhancement is several times larger, about 2.5 percent, than the precision inherent in our measurements, ± 0.6 percent.

8. The Rigid Hard Sphere Calculations

In order to look at the proposed enhancement from a different point of view we note that Dymond [9] in applying the

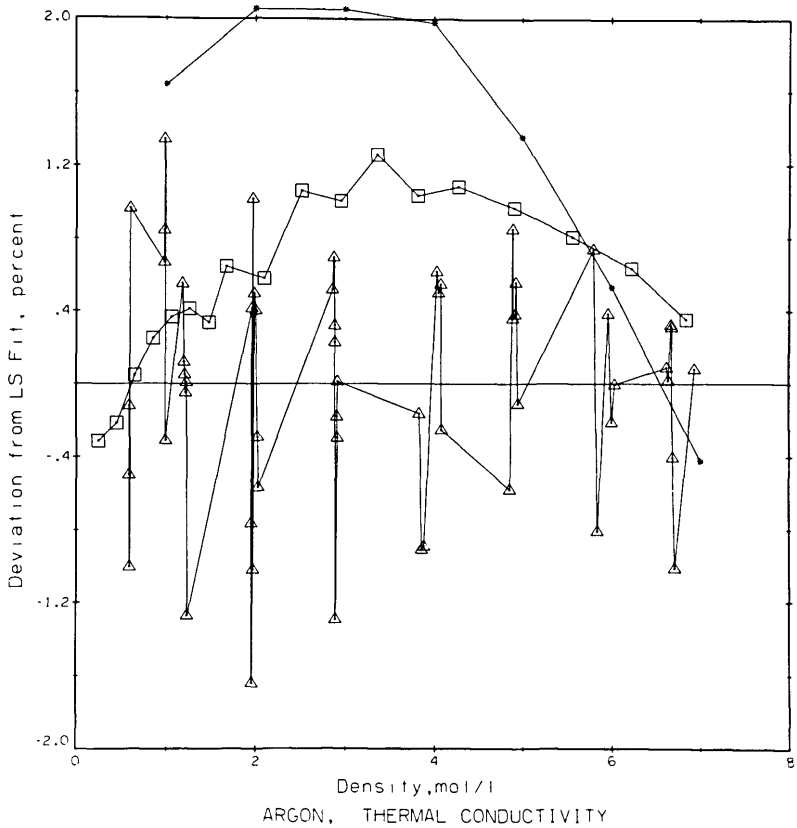

FIGURE 7. Deviations of the curve fit of equation 10 for the low density range only vs. density. △ this paper, ⊡ Kestin, et al. [2], * Hanley, et al. [22]. The error band of this fit is $\sigma = 0.51$ percent.

TABLE 4. *Coefficients of Least Squares Fittings*

Equation	Density Range of Fit mol/L	a_0 W/m•K	a_1 W•L/m•K•mol	a_2 W•L²/m•K•mol²	Average Deviation From Fit, Percent
10	0-20	$0.18089\times10^{-1}\pm0.16\times10^{-3}$	$0.63372\times10^{-3}\pm0.41\times10^{-4}$	$0.58497\times10^{-4}\pm0.20\times10^{-5}$	for 112 points 0.92
10	0-7	$0.17836\times10^{-1}\pm0.12\times10^{-3}$	$0.69942\times10^{-3}\pm0.82\times10^{-4}$	$0.62858\times10^{-4}\pm0.11\times10^{-4}$	for 56 points 0.51
		Fixed	Variable, B W•L/m•K•mol	Variable, C W/m•K	(Number of Points Fitted is 63)
11	0-5 and 15-20	A=0.01783 W/m•K D=0.060 L/mol	$-0.31015\times10^{-3}\pm0.38\times10^{-4}$	$0.18511\times10^{-1}\pm0.35\times10^{-3}$	for 63 points 0.54 for 112 points 0.88

hard sphere theory to dense and dilute gases, found evidence that the thermal conductivity data of argon and krypton shows an enhancement for temperatures up to 1.7 T_c which could not be represented by theory. We thus decided to apply the Van der Waals model to our data to see if a similar discrepancy could be noted at even higher temperatures. Use of the hard sphere model satisfies one of the considerations above, it supplies a functional form that is appropriate, yet highly constrained.

The Van der Waals model for transport properties of fluids is equivalent to a hard sphere model with a slightly temperature dependent hard core diameter, $\sigma_{HS}(T)$. It is a model that corrects Enskog's [23] expressions for the density dependence of the transport properties of a hard sphere fluid for both velocity correlations in the dense gas and for the attractive forces important in dilute gas collisions [9-11].

Enskog [23] based his equations on the assumption of molecular chaos and arrived at a value for the dense gas thermal conductivity given by:

$$\frac{\lambda_E}{\lambda_o} = \frac{1}{g(\sigma)} + 1.2\left(\frac{b}{V}\right) + 0.755\, g(r)\left(\frac{b}{V}\right)^2 \qquad (12)$$

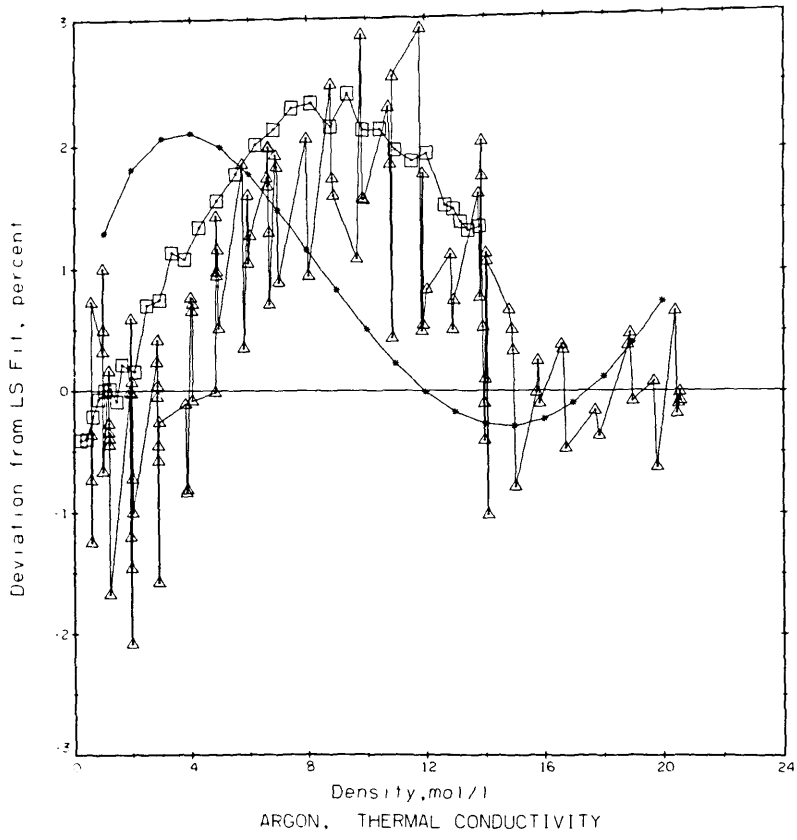

FIGURE 8. Deviations of the curve fit of equation 11 vs. density. The actual fit is limited to values between 0 and 5 mol/L as well as values between 15 and 20 mol/L. △ this paper, ⊡ Kestin. et al. [2], * Hanley, et al. [22].

where λ_o is the thermal conductivity of the low density gas of hard spheres, given by

$$\lambda_o = \frac{75}{64}\left(\frac{K^3 T}{\pi m}\right)^{1/2} \frac{1}{\sigma_{HS}^2} \tag{13}$$

$g(\sigma)$ is the radial distribution function at contact. For a system which can be approximated as given by Alder, et al. [11] the $g(\sigma)$ becomes

$$g(\sigma) = \frac{(1 - y/2)}{(1 - y)^3} \tag{14}$$

with

$$y = \frac{b}{4V} = \frac{1}{6}\pi \frac{N}{V}\sigma_{HS}^3 \tag{15}$$

the other symbols have the usual meaning.

Dymond [9] found that for high densities, where $\frac{V_o}{V} > 0.3$, V_o being the closed packed volume ($V_o = N\sigma_{HS}^3/2$), the Enskog values should be corrected for the molecular correlated motions and using molecular dynamics formulation he obtained

$$\left(\frac{\lambda}{\lambda_E}\right)_{MD} = 1.02 + 0.1\left[\frac{V_o}{V} - 0.3\right]; \frac{V_o}{V} > 0.3 \tag{16}$$

For the dilute and dense gas the expression has to be modified because the attractive forces do play an important role in heat conduction. Dymond [10] arrived at an expression, a function of the ratio T_c/T that it is supposed to account for the effect, the full expression being

$$\frac{\lambda_{HS}}{\lambda_E} = \left(\frac{\lambda}{\lambda_E}\right)_{MD} - \left[0.355 - 2.0\left(\frac{V_o}{V}\right) + 2.7\left(\frac{V_o}{V}\right)^2\right]\left(\frac{T_c}{T}\right)^{1/2}$$

$$\text{for } \frac{V_o}{V} < 0.3 \tag{17}$$

We have applied equations (12) to (17) to calculate the thermal conductivity of argon at $T = 300.65$ K as a function of

density, using a value of $V_o = 3.299 \times 10^{-4}$ m³/kg interpolated from Dymond's data of V_o as a function of temperature [10].

Figure 9 shows the comparison between our smoothed experimental thermal conductivity values and the values predicted by the hard sphere theory, λ_{HS} as a function of the ratio V_o/V. It can be seen that theory predicts the thermal conductivity of argon to within 0.7 mW/m•K (about 3.5 percent at low densities and 1.5 percent at high densities).

Figure 10 shows the difference between λ_{exp} and λ_{HS} as a function of density and it can be seen that the critical enhancement in the experimental data occurs near the critical density.

This comparison seems to support the existence of a critical enhancement in thermal conductivity even at temperatures around twice the critical temperature, a result that can only be detected if the accuracy of the thermal conductivity measuring method is sufficiently high.

9. Conclusions

This paper presents experimental data of the thermal conductivity of argon at 300.65 K from low density to 68 MPa obtained with a transient hot wire instrument.

The precision of the measurements is ± 0.6 percent while the accuracy of the data is estimated to be ± 1.0 percent. However, an Eucken factor of 1.0029 was obtained.

A small critical enhancement of about 2.5 percent was found in the experimental data between 0.34 ρ_c and 1.13 ρ_c, that has not been reported before. Comparison with values calculated from the hard sphere model shows that this model cannot predict the enhancement.

Our results agree with those of Kestin, et al. [2], Michels, et al. [12] and Le Neindre, et al. [13] within the mutual uncertainty.

The results confirm that the instrument is capable of measuring thermal conductivity of dense fluids with an accuracy of ± 1.0 percent. We expect to report results on helium, oxygen and propane in the near future.

One of us (CANC) is grateful for and wishes to acknowledge financial support from NATO Grant 1874 and would also like to thank the Luso-American Cultural Commission for a Fulbright-Hays travel grant. Our work was partially supported by NASA under Purchase Request C-32369-C.

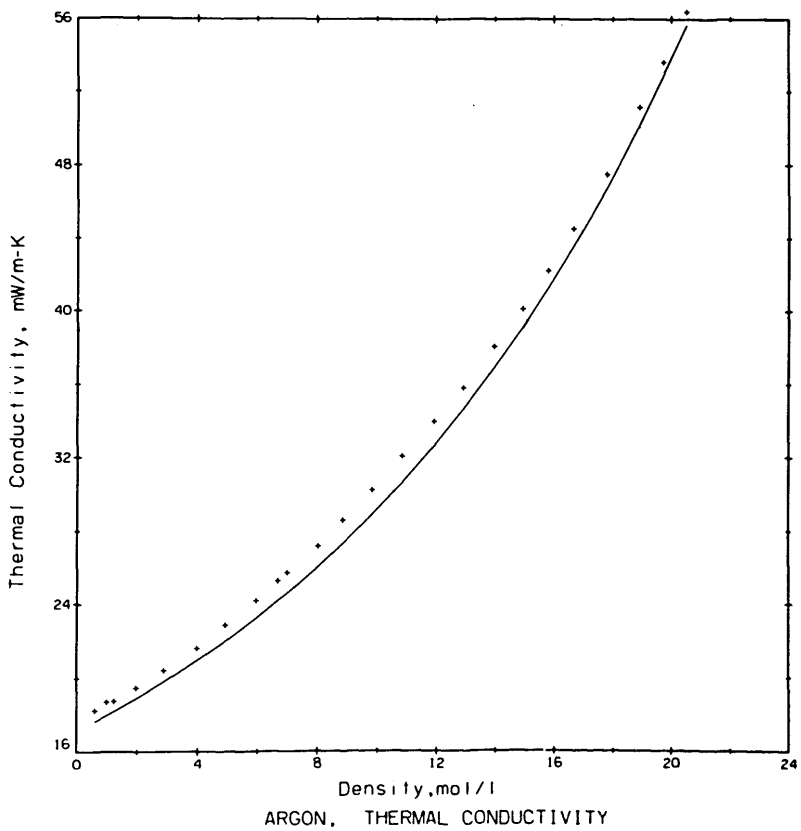

FIGURE 9. Calculated hard sphere and smoothed experimental thermal conductivities vs. density.

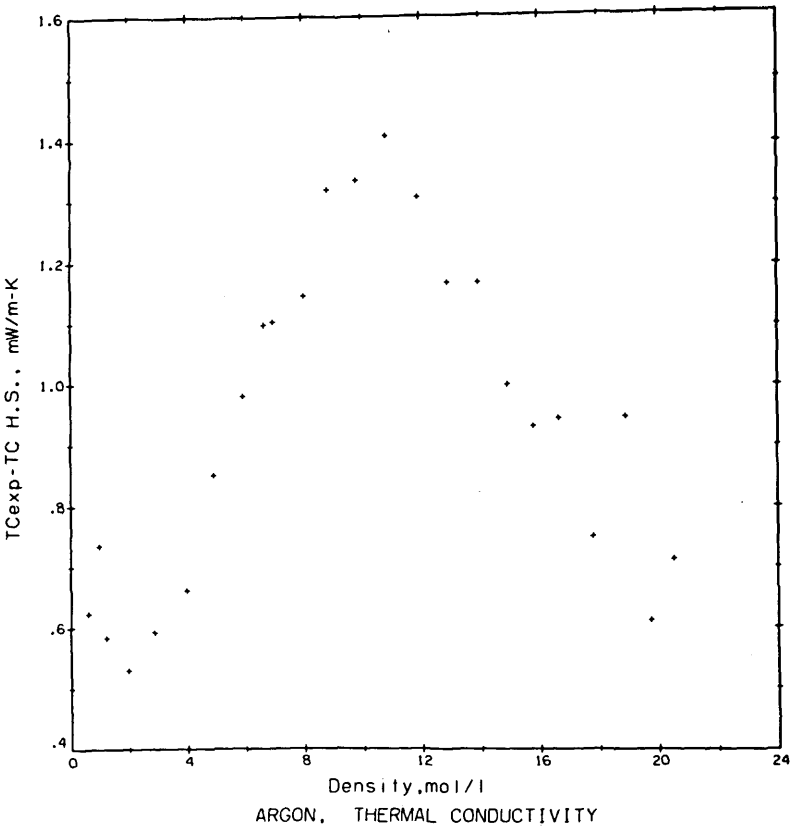

FIGURE 10. Differences between smoothed experimental and calculated hard sphere thermal conductivities vs. density.

10. References

[1] Healy, J. J.; de Groot, J. J.; Kestin, J. The theory of the transient hot-wire method for measuring thermal conductivity. Physica. **82C**(2): 392-408; 1976 April.

[2] Kestin, J.; Paul, R.; Clifford, A. A.; Wakeham, W. A. Absolute determination of the thermal conductivity of the noble gases at room temperature up to 35 MPa. Physica. **100A**(2): 349-369; 1980 February.

[3] Assael, M.J.; Dix, M.; Lucas, A.B.; Wakeham, W.A. Absolute determination of the thermal conductivity of the noble gases and two of their binary mixtures. J. Chem. Soc., Faraday Trans. **77**(1): 439-464; 1981.

[4] de Castro, C. A. Nieto; Calado, J. C. G.; Wakeham, W. A. Absolute measurements of the thermal conductivity of liquids using a transient hot-wire technique. Cezarilyan, A. ed. Proceedings of the seventh symposium on thermophysical properties; 1977 May 10-12; Gaithersburg, Maryland; New York; ASME; 1977; 730-738.

[5] de Castro, C. A. Nieto; Calado, J. C. G.; Wakeham, W. A. Thermal conductivity of organic liquids measured by a transient hot-wire technique. High Temperatures-High Pressures. **11**: 551-559; 1979.

[6] Menashe, J.; Wakeham, W. A. Absolute measurements of the thermal conductivity of liquids of pressures up to 500 MPa. to be published, Physica.

[7] Roder, H. M. A transient hot wire thermal conductivity apparatus. to be published, J. Res. Nat. Bur. Stand. (U.S.).

[8] Kestin, J.; Ro, S. T.; Wakeham, W. A. Viscosity of the noble gases in the temperature range 25-700 °C. J. Chem. Phys. **56**(8): 4119-4124; 1972 April 15.

[9] Dymond, J. H. The interpretation of transport coefficients on the basis of the van der Waals model. I. Dense fluids. Physica. **75**: 100-114; 1974.

[10] Dymond, J. H. The interpretation of transport coefficients on the basis of the van der Waals model. II. Extension to dilute gases. Physica. **79A**(1): 65-74; 1975 January-March.

[11] Alder, B. J.; Gass, D. M.; Wainwright, T. E. Studies in molecular dynamics. VIII. The transport coefficients for a hard sphere fluid. J. Chem. Phys. **53**(10): 3813-3826; 1970 November 15.

[12] Michels, A.; Sengers, J. V.; Van de Klundert, L. J. M. The thermal conductivity of argon at elevated densities. Physica. **29**: 149-160; 1963.

[13] Le Neindre, B.; Bury, P.; Tufeu, R.; Johannin, P.; Vodar, B. Recent developments at Bellevue on thermal conductivity measurements of compressed gases. Flynn, D. A.; Peavy, B. A., Jr. ed. Thermal conductivity; Proceedings of the seventh conference; 1967 November 13-16; Gaithersburg, Maryland. Nat. Bur. Stand. (U.S.) Spec. Publ. 302; 1968 September. 579-593.

[14] Haarman, J. W. Thesis. Technische Hogeschool; Delft; 1969.

[15] de Groot, J. J.; Kestin, J.; Sookiazian, H. Instrument to measure the thermal conductivity of gases. Physica. **75**: 454-482; 1974.

[16] de Castro, C. A. Nieto; Calado, J. C. G.; Wakeham, W. A.; Dix, M. An apparatus to measure the thermal conductivity of liquids. Journal of Physics E: Scient. Inst. **9**: 1073-1080; 1976.

[17] Mani, N. Precise determination of the thermal conductivity of fluids

using absolute transient hot-wire technique. Thesis. University of Calgary. Calgary, Alberta, Canada. 1971 August.

[18] Goodwin, R. D. Apparatus for determination of pressure-density-temperature relations and specific heats of hydrogen to 350 atmospheres at temperatures above 14°K. J. Res. Nat. Bur. Stand. (U.S.) **65C**(4); 231-243; 1961 October-December.

[19] de Castro, C. A. Nieto; Wakeham, W. A. Experimental aspects of the transient hot-wire technique for thermal conductivity measurements. Mirkovich, V. V. ed. Thermal conductivity 15. 1977 August 24-26; Ottawa, Ontario, Canada; New York; Plenum Publ. Corp.; 1978; 235-243.

[20] Kestin, J.; Wakeham, W.A. A contribution to the theory of the transient hot-wire technique for thermal conductivity measurements. Physica. **92A**(1 & 2): 102-116; 1978 June.

[21] An equation of state for argon, based on the work of Gosman, A. L.; McCarty, R. D.; Hust, J. G. Thermodynamic properties of argon from the triple point to 300 K at pressures to 1000 atmospheres. Nat. Bur. Stand. (U.S.) Nat. Stand. Ref. Data Ser. 27; 1969 March. 146 p. The functional form of the equation and the pertinent coefficients are given in reference 22.

[22] Hanley, H. J. M.; McCarty, R. D.; Haynes, W. M. The viscosity and thermal conductivity coefficients for dense gaseous and liquid argon, krypton, xenon, nitrogen and oxygen. J. Phys. Chem. Ref. Data. **3**(4): 979-1017; 1974.

[23] Enskog, D. Kinetische Theorie der Wärmeleitung, Reibung und Selbstdiffusion in gewissen verdichteten Gasen und Flüssigkeiten. Kungl. Svenska Vetenskapsakademiens Handlingar. **63**(4): 1-44; 1922.

JOURNAL OF RESEARCH of the National Bureau of Standards
Vol. 86, No. 3, May-June 1981

The Effect of Calcium Carbonate on the Stability of Acid Treated Papers

E.L. Graminski* and E.J. Parks**

National Bureau of Standards, Washington, DC 20234

December 17, 1980

Exposure of kraft wood pulps to an acidic medium results in a destabilization of wood pulp. The degree of destabilization appears to depend on the concentration of acid the pulp is exposed to. The addition of calcium carbonate to acid destabilized pulp does not restore the pulp to its original stability. The absorption of alkali metals is pH dependent which could explain the destabilization of wood pulps when exposed to an acid medium. A number of questions arise about the merit of stabilizing degraded paper documents by deacidification with alkaline earth salts and the usefulness of an alkaline reserve in paper.

Key words: Alkaline reserve; cellulose stabilizers; paper deacidification; paper destabilization; paper permanence; pH history

1. Introduction

Concern over the instability of paper has continued for more than 100 years. In a book published in 1824, the author lamented over the condition of paper in books that were less than 10 years old. [1][1] If that were noted today, it would most likely be assumed that the manufacture of paper from wood pulp was to blame. In 1824, it was the formidable rag paper that proved to be unstable. Nevertheless, paper can be made to last for centuries or millenia. In evidence is the fact that many books, centuries old, are still in excellent condition.

The stabilization of paper is a matter of enormous worldwide economic and cultural impact, and efforts have been made for at least fifty years on the one hand to determine causes of paper instability and on the other to evaluate the longevity of paper by means of accelerated aging. The earliest experiments in accelerated aging involved placing paper in an oven at 100 to 105 °C for times ranging from 20 to 125 h [2,3]. The classification of paper permanence was based on the retention of the original properties of unaged paper. If a paper subjected to accelerated aging manifested a high retention of physical properties, it was considered permanent, while papers that manifested considerable decline in properties were considered to be impermanent. No attempts were made to predict the "natural" lifetime of paper, and until recently, data were not available for meaningful comparisons of accelerated and long-term aging, necessary to evaluate the former.

The accelerated aging studies did indicate that exposure of pulp to excessive acidity resulted in an unstable manufactured product [4]. The origin of most of the acid was aluminum sulfate, which was used to size paper with rosin. Aluminum sulfate hydrolyzes in water to produce sulfuric acid. A later study showed that the aluminum ion was selectively retained by pulp fibers [5]. More recently, Parks [6] inferred, on the basis of thermoanalytic data, that the aluminum ion, interacting with carboxyl groups in cellulose, might be a contributing cause for the instability of paper. Parks *et al* [7, 8, 9] showed that large amounts of organic acid were generated during the humid accelerated aging of unstable, weakly acidic paper, and that the amounts of acid generated were correlated with changes in physical properties and color reversion. Their data did not indicate catalysis of aging by the generated acid.

Prior accelerated aging tests had demonstrated that paper filled with calcium carbonate possessed considerable stability [10]. An investigation of naturally aged paper produced further evidence for the stabilizing effect of calcium carbonate [11], supporting the rationalization that initially acid papers were unstable because of acid hydrolysis and that alkaline papers, conversely, are stable. It was further reasoned that treatment of degraded, acidic paper documents with calcium alkali would neutralize acidity and arrest further acid-catalyzed degradation [12].

*Current address: 201-3A, Bureau of Engraving and Printing, 14th & C St. SW, Washington, DC 20228

**Center for Materials Science, National Measurement Laboratory

[1]Figures in brackets indicate literature references at the end of this paper.

With one exception [11], all of the information on the relationship of paper stability and alkalinity was derived from an accelerated aging test that consisted of placing paper specimens in an oven at 100 °C for 72 hours [13]. The validity of accelerated aging at a single temperature itself is questionable because of demonstrated differences in the temperature dependence of the degradation rate constants for different papers [14]. Furthermore, Graminski *et al* [15] recently have shown that the deterioration rate of properties closely related to the tensile strength of paper is directly proportional, in an accelerated aging test at a given temperature, to the moisture content of the paper. When one considers the low relative humidity of the atmosphere in an oven at 100 °C, even when the relative humidity of the surrounding environment is high, it is easy to infer that little fiber degradation occurs under these circumstances, and that oven aging must be fundamentally incomparable with natural aging.

As an added source of confusion, however, many workers have observed appreciable declines in folding endurance and internal tearing resistance during oven aging. Functional groups, introduced during pulp manufacturing and especially during bleaching, react to form cross-links. As the number of cross-links increases, wet strength increases and fiber flexibility decreases. The decreased fiber flexibility results in decreases in folding endurance [8].

Unless paper contains an adequate amount of water, it must be assumed that the three main degradative reactions—cross-linking, hydrolysis, and oxidation [7, 8, 9]—can occur in different ratios than in natural degradation. Thus, the assessment of "real" permanence would lack a valid theoretical correlation with dry aging at a high temperature.

Wilson and Parks [16] recently compared the changes in 18 papers after three days of oven aging at 100 °C with changes observed after 36 years of natural aging in an office in which the relative humidity varied over the years. Considering all 18 papers as a group, the correlation between accelerated aging under these conditions and uncontrolled "natural" aging was not high. Comparisons between various subsets generated higher correlations, but the decline of physical properties in some papers was lower after 36 years of natural aging than after three days of oven aging, while the reverse was true for other papers.

However, their data indicate an interesting correlation between head box pH and retention of folding endurance after natural aging: the higher the head box pH, the greater the retention of folding endurance. The coefficient of correlation between the head box pH and retention of folding endurance for two sets of acid wood pulp papers was 0.92 and 0.99. The coefficient of correlation for one set of rag papers was somewhat lower at 0.86. In addition, their data show an excellent correlation between head box pH and the wet strength of the paper, observed after 36 years of natural aging and expressed as a percent of dry strength. The coefficient of correlation for each of the two sets of acid wood pulp papers was 0.99 and for the rag papers it was 0.97. These data suggest the previously unevaluated hypothesis that the pH "history" of a pulp affects the permanence of paper made from it.

In the present investigation, aging was conducted to determine whether the addition of calcium carbonate would impart resistance to humid aging, to paper previously subjected to acid extraction. Pulps were treated with dilute mineral acid and aluminum sulfate to impart instability. Subsequent treatment with calcium carbonate produced alkaline handsheets. The handsheets were subjected to accelerated aging at 90 °C and 50 percent R. H., in order to indicate whether the addition of the alkaline salt, calcium carbonate, to a destabilized pulp result in a paper fully stabilized against aging under humid conditions.

2. Experimental Procedure

2.1. Samples

Handsheets were prepared from a northeastern bleached kraft pulp containing approximately 85 percent alpha cellulose and 15 percent hemicellulose. Handsheets which were prepared from the pulp as received (untreated) were made in tap water. All other handsheets were prepared in distilled water (table 1). The handsheets were stored in a chamber controlled at 35 °C and 90 percent relative humidity for at least 18 h to relieve any stresses which may have formed during the preparative stages.

The "deashed" handsheets were made from demineralized pulp. Pulp was torn into pieces approximately two square inches and soaked in 0.1 N hydrochloric acid at a five percent consistency. After one hour, the acid was drained and fresh acid was added to the pulp. After the fourth acid treatment, the pulp was washed with distilled water on a large Buchner funnel until the pH of the filtrate was identical to the pH of the distilled water and remained at that pH for an additional three to four rinses.

Aluminum treated handsheets were prepared from the deashed pulp after treatment with 0.1 M calcium acetate. Following four one-half hour treatments with 0.01 M aluminum sulfate, the treated pulp was washed extensively.

Beating of pulps was done in a laboratory mill at 10 percent consistency with no clearance between bedplate and roll for 4,000 revolutions at 3.33 N (.34 kg force) and a relative velocity of roll to bedplate of 6 m/sec. With the exception of the untreated pulp, beating was done in distilled water using sufficient wet pulp to provide 40 g of the dry pulp for each charge. If several charges were used, they were placed in a large stainless steel container, diluted to

approximately one percent consistency and blended for approximately one hour prior to preparing handsheets.

Aliquots, containing sufficient pulp to make a 30.5 x 30.5 cm handsheet having a weight of 70 g/m² ±5 percent, were placed in a British Disintegrator (see TAPPI Standard T205os-71), diluted with distilled water to a consistency of approximately 0.5 percent and disintegrated for 3,000 revolutions. The disintegrated pulp was placed in a 30.5 x 30.5 cm deckle box containing approximately 28 L of distilled water. The contents were agitated by moving a perforated plate up and down five times, followed by a pause of approximately 10 seconds, then drained through a 100 mesh monel wire screen. The wire containing the formed sheet was placed on a blotter, covered with wool felt and consolidated by pressing with a 33 cm long roller weighing 22.5 kg. The sheet was carefully removed from the wire, placed between wool felts and passed through a roll press at a pressure of approximately 7 kg/linear cm. The pressed sheet was then dried on a drum dryer at 95 °C for approximately four minutes. The tension on the endless felt of the drum dryer was adjusted to restrict shrinkage to a minimum. The sheets were stress relieved by suspending them in a humidity chamber at 35 °C and 90 percent relative humidity for approximately 16 hours.

If the handsheets were to be filled with calcium carbonate, 0.65 g $CaCO_3$ was added to the distilled water in the deckle box and dispersed. Disintegrated pulp was then added, stirred and allowed to equilibrate for one minute before the water was drained. The remainder of the handsheet preparation procedure was as described above.

A number of handsheets also were prepared from aluminum sulfate treated pulp which was in contact with the $CaCO_3$ for one hour before forming into a handsheet. The purpose of this procedure was to determine whether the contact time with the $CaCO_3$ affected the stabilization of paper.

2.2 Accelerated Aging

Constant temperature oil baths were constructed of stainless steel. An immersion heater controlled by a relay box and thermoregulator provided the principal source of heat with a desired temperature control to ± 0.1 °C. A heating coil, immersed in the bath, was an auxiliary source of heat, with current input controlled by a variable transformer. The oil was continuously pumped in the bath with an immersion type pump to ensure uniform temperature distribution.

Two baths in series, maintained at 75 °C and 90 °C, were equipped with prehumidifiers and aging vessels, respectively. To provide a vented atmosphere of 50 percent relative humidity in the aging vessels, about 50 cm of gas per minute was metered through water and saturated in the prehumidifier at 73 °C , passed through glass tubing surrounded by a heating jacket at a temperature somewhat higher than 73 °C to avoid condensation, then through coiled glass tubing immersed in the second bath at 90 °C, and finally through the aging vessel containing suspended paper specimens. The baths were covered with black cloth to exclude light.

Humid air at 50 percent relative humidity and 90 °C contains about 14 percent oxygen gas, 30 percent moisture and 56 percent nitrogen gas. In order to obtain a humid atmosphere containing about 20 percent oxygen gas, a mixture of 30 percent oxygen gas and 70 percent nitrogen was substituted for air and was saturated at 73 °C. According to calculations based on published tables, this gas contained about 20 percent oxygen.

Aging periods of 1, 3, 6, 12, and 24 days were selected to provide information at various degress of degradation. In some cases the one day period or the three day period was omitted.

2.3 Properties Investigated

The following properties were investigated, using the listed TAPPI test methods: *Folding Endurance* T511 Sn-69, *Brightness* T452 OS-58, *Alkaline Solubility* T212 OS-54, *Copper number* T430 M-52, *Tensile Strength* T494 OS-70 using 1.5 cm wide specimens at a span of 10 cm and a rate of elongation of 1 cm/min., and *pH* by method T509 SU-68 with the exception that the pH measurement was made on the decantate.

Internal tear was performed on an Elmendorf tear tester having a 200 g capacity. A single ply was used unless the tear strength deteriorated considerably, necessitating three or four plies in order to obtain a reading in the range suggested for the instrument.

Zero span tensile strength was determined with the aid of specially designed commercial zero span clamps which were attached to a commercial constant rate of elongation tensile tester. The rate of elongation was 0.3 mm/minute.

Wet tensile strength was determined on a constant rate of elongation tensile tester using specimens 1.5 cm wide and 10 cm long. The samples were soaked for two hours in distilled water prior to testing.

Moisture regain specimens were first conditioned in a desiccator for 24 hours and then exposed to an atmosphere maintained at 23 ± 1 °C and 50.0 ± 2.0 percent relative humidity for at least 24 hours. Specimens of approximately two grams were placed in weighing bottles and the total weight was determined to the nearest 0.1 mg. The sample was then dried in a vacuum oven at 105 °C for one hour, covered immediately upon opening the oven, cooled in a desiccator for two hours, and reweighed. This procedure was repeated until changes in weight were no longer observed. The specimen was then removed from the weighing bottle, and the empty bottle was dried in the vacuum oven

at 105 °C for one hour, cooled in a desiccator for two hours and weighed. The difference between the weight of the bottle containing the dried specimen, and the empty weighing bottle was the weight of the anhydrous. specimen. The weight of water divided by anhydrous specimen multiplied by 100 was the percent moisture regain.

Aluminum was determined in ash by the p-hydroxyquinoline complexation method (17). Calcium in ash was titrated in reacted solution with EDTA, using cal-red indicator (18).

The results for folding endurance and zero span tensile strength are given in tables 2 and 3 and represent the averages for 8 to 12 specimens. The results of these two properties are representative of all the other properties investigated. The results for the remaining properties are not given.

3. Discussion

Two factors, critical in accelerated aging studies of paper, are not considered in the present investigation: (1) the temperature dependence of degradation rate constants, and (2) effects of moisture on degradation rates. Since the accelerated aging conditions were identical, and closely controlled, and since each set of handsheets was prepared from a single batch of pulp, the effect of treatments on the pulp stability under these controlled conditions can be readily assessed.

The untreated pulp (table 1) was comparatively stable during humid accelerated aging tests over the time spans indicated. Minimal decline in the zero span tensile strength indicates that fibers did not experience serious degradation (table 2). Relatively slow increases in wet strength (table 3) and decreases in folding endurance (table 4) further differentiate this paper from the less stable modifications.

Demineralization with dilute acid resulted in a remarkable decrease in stability. The wet strength of deashed paper increased rapidly during the early stages of humid aging (table 3 and figure 1), reached a maximum and then rapidly declined over the remaining aging interval. Treatment of the deashed pulp with aluminum sulfate resulted in little or no additional effect on the degradation rate (tables 2-4 and figure 2). These data do not support Parks' inference (6) that aluminum destabilized paper, as the aluminum treated paper is not less stable than the deashed paper from which it was prepared.

The addition of calcium carbonate to either the deashed or aluminum-treated paper appears to retard the deterioration process. The increase in wet strength is much slower at the onset of aging. In fact, the changes in wet strength with time initially are only slightly different from those of the untreated paper. $CaCO_3$-filled paper reaches a maximum and then, unlike untreated paper, declines over the remaining interval of aging. The rate of decline of zero span tensile strength and that of folding endurance decreased also when calcium carbonate was added to either deashed or aluminum-treated pulp, but the rate of deterioration still was

TABLE 1. *Description of Samples*

Pulp Treatment	Mass Per Unit Area (g/m^2)	Thickness (mm)	pH Cold	pH Hot	Ash Content (%)	Aluminum Content (meq/100g)	Calcium Content (meq/100g)
None	78	.134	6.18	6.17	0.112	—	2.5
Deashed	75	.138	4.93	5.04	0.006	—	—
Deashed + $CaCO_3$	78	.145	7.98	8.70	—	—	62
Aluminum Treated	68	.145	5.22	4.68	0.141	3.12	—
Aluminum Treated + $CaCO_3$ (1 minute)	70	.150	7.80	8.80	—	3.35	67
Aluminum Treated + $CaCO_3$ (1 hour)	73	.142	7.88	8.52	—	1.5	33

TABLE 2. *Effect of Aging at 90°C and 50 Percent Relative Humidity on Folding Endurance (Double Folds Under 1 kg of Tension)*

Pulp Treatment	Aging Time, Days					
	0	1	3	6	12	24
	Double Folds					
None	1890	1800	—	1610	1510	500
Deashed	1390	970	830	21	0	0
Deashed + $CaCO_3$	1460	1080	870	430	11	0
Aluminum Treated	960	—	52	2	0	0
Aluminum Treated + $CaCO_3$ (1 minute)	970	—	623	410	61	0
Aluminum Treated + $CaCO_3$ (1 hour)	1330	—	728	326	5	0

much greater than observed in paper made from untreated pulp (tables 2 and 4). Increasing the contact time of the calcium carbonate with the aluminum-treated pulp did not appear to influence the degradation rate, even though one-half of the aluminum was displaced (table 1).

The results of this investigation suggest that destabilization occurs when pulps come into contact with an acid medium. Since treatment of deashed pulp with calcium carbonate does not restore the pulp to its original stability, it is evident that neither the presence of calcium nor the alkalinity of calcium carbonate is sufficient to ensure stabilization of the acid-modified pulp.

Since alkaline papers are frequently stable, however, we suggest that the pH history of a pulp, particularly whether or not the pulp is exposed to acid media at critical points in the paper making process, is more important to permanence than the final pH of the paper. This hypothesis would be consistent with either modification of the unaged pulp by acid treatment, or extraction of a substance under acid conditions—e.g., trace metals—that is capable of effecting stabilization. Restoration of stability then would occur only if the effect of acid extraction could be reversed, e.g., by returning the same trace metals to the fibers.

In view of the limited improvement conferred by calcium carbonate to pulp destabilized by contact with acid, possible side reactions that may result from deacidification of deteriorated documents assume greater importance. The purpose in treating degraded, acid paper is to neutralize the acid and arrest further degradation due to acid hydrolysis. However, alkaline hydrolysis under these conditions is a disturbing possiblity.

During natural degradation, paper undergoes oxidation to some extent. Cellulose oxidized with formation of one or more alkoxy groups at the 1-, 3-, or 6-position of the anhydroglucose ring. In alkaline media, the possibility arizes of rapid elimination of an alkoxyl group, resulting in chain scission with the formation of one reducing and one nonreducing end group [19]. The reducing group would further oxidize to carboxylic acid. Therefore an old document, after extensive oxidation, could actually suffer alkali-catalyzed degradation during the deacidification process, this risk increasing with the strength of the alkalinity of the medium.

4. Conclusion

Extraction of pulp with mineral acid (deashing) severely reduces the resistance of paper manufactured from such pulp to accelerated aging under humid conditions. Addition of aluminum ion does not further diminish the stability of deashed pulp. Addition of calcium carbonate to acid-

TABLE 3. *Effect of Aging at 90°C and 50 Percent Relative Humidity on Zero Span Tensile Strength, Expressed as Km of Paper*

Pulp Treatment	Aging Time, Days					
	0	1	3	6	12	24
	Breaking Length, Km					
None	14.7	14.9	—	14.8	14.2	12.1
Deashed	14.2	12.9	10.4	7.7	3.8	0.9
Deashed + $CaCO_3$	13.3	13.0	13.0	12.2	9.0	3.4
Aluminum Treated	12.9	—	10.0	6.3	3.8	1.1
Aluminum Treated + $CaCO_3$ (1 minute)	13.0	—	12.7	12.3	10.4	5.9
Aluminum Treated + $CaCO_3$ (1 hour)	13.0	—	12.5	11.3	8.1	2.0

TABLE 4. *The Degradation Rates for Zero Span Tensile Strength and Folding Endurance of Various Papers at 90°C and 50 Percent Relative Humidity*

Pulp Treatment	$\frac{\Delta [\log \text{Z.S.T.}]}{\Delta T \text{ (days)}} \times 10^3$	$\frac{\Delta [\log \text{Fold}]}{\Delta T, \text{ days}} \times 10^3$
None	4	23
Deashed	51	298
Deashed + $CaCO_3$	25	174
Aluminum Sulfate Treated	44	447
Aluminum Sulfate Treated + $CaCO_3$ (1 minute)	15	123
Aluminum Treated + $CaCO_3$ (1 hour)	23	206

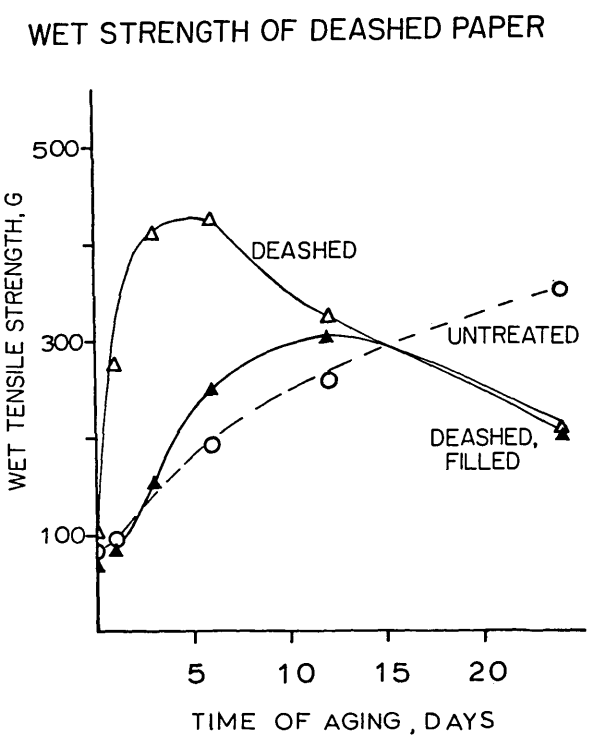

FIGURE 1. *Generation of wet strength in untreated-, deashed-, and $CaCO_3$ filled deashed paper as a function of time at 90 °C and 50 percent relative humidity.*

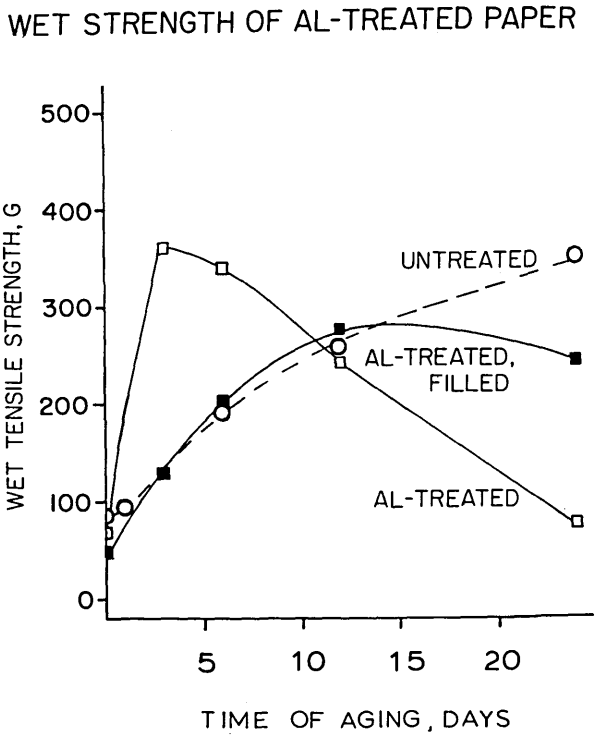

FIGURE 2. *Generation of wet strength in untreated-, Al-treated, and $CaCO_3$-filled Al-treated paper as a function of time at 90 °C and 50 percent relative humidity.*

TABLE 5. *Effect of Aging at 90°C and 50 Percent Relative Humidity on Wet Tensile Strength, Grams*

Pulp Treatment	Aging Time, Days					
	0	1	3	6	12	24
	Wet Tensile Strength, Grams					
None	82	95	—	191	258	350
Deashed	104	277	415	427	323	206
Deashed + $CaCO_3$	67	83	154	249	301	205
Aluminum Treated	81	—	362	340	241	97
Aluminum Treated + $CaCO_3$	43	—	30	203	277	242

deashed pulp causes the paper to be alkaline and only partially restores the resistance to aging that is lost on acid extraction.

Consideration of data found in the literature, in conjunction with the current data, suggest the hypothesis that paper is rendered unstable by acid extraction of undetermined stabilizers, and that stability is not fully restored merely by adding an alkaline salt to the pulp. Hence the pH history of the pulp, particularly whether it is exposed to acid during manufacture acquires great importance.

The practice of deacidifying old documents with alkaline salts needs to be considered in the light of possible damage to such documents by hydrolytic cleavage of β-alkoxyl groups, catalyzed by alkaline media.

5. References

[1] Murray, John. Observations and experiments on the bad composition of modern paper, with the desorption of a permanent writing ink which cannot be discharged. London: G. and W. B. Whitaker; 1824.

[2] Hall, G. Permanence of paper. Paper Trade Journal **82** (14): 185–191; 1926 April.

[3] Rasch, R. H. A study of purified wood fibers as a papermaking material. J. Res. Nat. Bur. Stand. (U.S.). **3**: 469–506. 1929 February.

[4] Rasch, R. H.; Shaw, M. B.; Bicking, G. W. Highly purified wood fibers as papermaking materials. J. Res. Nat. Bur. Stand. (U.S.). **7**: 765–782; 1931 August.

[5] Launer, H.F. Retention of aluminum ion and hydrogen ions in papers. J. Res. Nat. Bur. Stand. (U.S.). **23**: 663–674; 1939 December.

[6] Parks, E. J. Thermal analysis of modified cellulose. Tappi **54** (4): 537–544; 1971 April.

[7] Parks, E.J., Hebert, R. L. Accelerated aging of laboratory handsheets: changes in acidity, fiber strength, and wet strength NBS Report 10627, NTIS Com 75 10164; 1971 December. 42 p.

[8] Parks, E.J.; Hebert, R.L. Accelerated aging of laboratory handsheets: retention of folding endurance, internal tear, bursting strength, and tensile strength. NBS Report 10628. NTIS Com 75 10165; 1971 December. 68 p.

[9] Parks, E.J.; Hebert, R. L. Accelerated aging of laboratory handsheets: reflectance, moisture regain, sonic modulus, and differential thremal analysis. NBS Report 10687. NTIS Com 75 10162; 1972 February. 30 p.

[10] Shaw, M. B.; O'Leary, M. J. Effect of filling and sizing materials on stability of book papers. J. Res. Nat. Bur. Stand. (U.S.). **21**: 671–695; 1938 November.

[11] Hanson, F. S. Resistance of paper to natural aging. Paper World **20**: 1157–1163; 1939.

[12] Barrow, W.J. Deterioration of book stock, causes and remedies. Richmond, Virginia: Virginia State Library Publications; 1959. 70 p.

[13] TAPPI testing methods and recommeded practices. Effect of heating on folding endurance (Relative Stability of Paper). Suggested Test Method T 453 su-70. New York: Technical Association of the Pulp and Paper Industry; 1976.

[14] Gray, G. G. An accelerated aging study comparing kinetic rates vs. TAPPI Standard 453. Tappi **52** (2): 325–334; 1969 February.

[15] Graminski, E. L.; Parks, E. J.; Toth. E. E. The effects of temperature and moisture on the accelerated aging of paper. Eby, R. K., ed. Durability of Macromolecular Materials. Washington, D.C.: American Chemical Society Symposium Series 95; 1979. 342–355.

[16] Wilson, W. K.; Parks, E. J. Comparison of accelerated aging of book papers in 1937 with 36 years of natural aging. NBSIR 74–362. NTIS PB 246–554; 1974 December.

[17] Vogel A. I. *A Textbook of Quantitative Inorganic Analysis.* New York: John Wiley and Sons; 1961. p 386.

[18] Scandinavian pulp, paper and board testing committee. Calcium in pulp. Svensk Papperstidning **65**: 411; 1962.

[19] Isbell, H. S. Interpretation of some reactions in the carbohydrate field in terms of consecutive electron displacement. J. Res. Nat. Bur. Stand. (U.S.). **32**: 45–59; 1944 February.

JOURNAL OF RESEARCH of the National Bureau of Standards
Vol. 86, No. 3, May-June 1981

Properties of Labeling Methods for Determining Shortest Path Trees*

Douglas R. Shier† and Christoph Witzgall†

National Bureau of Standards, Washington, DC 20234

January 21, 1981

A number of labeling procedures for determining shortest paths in a network employ a sequence list in order to carry out the required steps systematically. This paper studies certain formal properties of such sequence lists. It is shown that the desirable property of branching out from nodes whose labels represent actual in-tree distances is assured for certain ways of managing the sequence list, but not for others. The relationship of this property to the computational complexity of various labeling procedures is also investigated.

Key Words: Complexity; labeling; network; sequence list; shortest path; tree

1. Introduction

A number of methods for finding shortest paths in networks have been proposed during the past 30 years. Stimulated to a great extent by the wealth of application areas in which shortest path calculations arise (notably in transportation planning models), considerable effort has been directed toward the efficient implementation of such methods for large-scale problems. Recent evidence [2, 11][1] indicates that a method proposed by Pape [11] is remarkably successful in practice. However, compelling reasons for the observed efficiency of Pape's method are lacking. One motivation for the present work is to find some formal justification for the success of Pape's method.

To begin, some necessary terminology and notation will be introduced. Consider a *directed network* (N, A) with *node set* N and *arc set* A, and let

$$I(a) \in N, J(a) \in N$$

denote the *origin* and *destination* of arc $a \in A$. Given a *length* $l(a)$ for each arc $a \in A$, the length $l(P)$ of any path P is defined to be the sum of its constituent arc lengths. A frequently encountered problem is that of finding, among all paths (if any) extending from $i \in N$ to $j \in N$, a *shortest path*: i.e., a path from i to j having minimum length. It is assumed that the network contains no closed paths with negative length, in order to guarantee that such shortest paths always exist.

If r is a given node of N, then shortest paths from r to all nodes j accessible (by a path) from r can be selected to form a *shortest path tree* with *root* r. That is, the unique path in this tree from node r to node j is in fact a shortest path between the nodes.

A tree T, rooted at node r, can be uniquely specified by a *predecessor map* q that assigns to each node $j \neq r$ in T its *predecessor arc* $q(j)$ in the tree. Similarly, each node $j \neq r$ in the tree has a unique *predecessor node* $p(j) = I(q(j))$ in the tree. The nodes $p(j), p(p(j)), \ldots, r$ constitute the *ancestors* of node j in the tree. The *branch* at node i of tree T, or $B(i,T)$, is the largest subtree of T rooted at i. Thus, $B(i,T)$ contains node i and all nodes j which have i as an ancestor.

*AMS Subject Classification: 05C35, 05C05

†Center for Applied Mathematics, National Engineering Laboratory

[1] Numbers in brackets indicate literature references at the end of this paper.

A number of methods for determining a shortest path tree with root r are based on providing a *labeling* (T,d), where T is a tree rooted at r in the network and $d\colon N \to R \cup \{\infty\}$ assigns a *label* $d(j)$ to each node j such that

$$d(j) = \infty \text{ for nodes } j \text{ not in } T. \tag{1}$$
$$d(i) + \ell(a) \leqslant d(j) \text{ for all arcs a} = (i,j) \text{ in } T. \tag{2}$$

If i is an ancestor of j in T, then $P(i,j)$ denotes the unique simple path in T from node i to node j. If (T,d) is a labeling, then repeated application of property (2) produces

$$d(i) + \ell(P(i,j)) \leqslant d(j) \tag{3}$$

for all nodes i,j in T with i an ancestor of j. In particular, if node j is in T then r is an ancestor of j, whence

$$d(r) + \ell(P(r,j)) \leqslant d(j). \tag{4}$$

Accordingly, $d(j) - d(r)$ is an upper bound on the length of the tree path from r to j. As a consequence, $d(j) - d(r)$ is also an upper bound on the length of a shortest path in the network from r to j.

A labeling (T,d) is said to be *optimal* if

$$d(r) = 0, \tag{5}$$
$$d(I(a)) + \ell(a) \geqslant d(J(a)) \text{ for all } a \in A. \tag{6}$$

A suitable interpretation of (6) is assumed in the case of infinite labels. If a labeling (T,d) is optimal, then T is a shortest path tree rooted at node r [5,14]. On the other hand, if T is a shortest path tree rooted at r, then the distances $d(j)$ from the root to node j define an optimal labeling (T,d).

If (T,d) is any labeling, and (6) is violated for some arc $a \in A$, then redefining

$$d(J(a)) = d(I(a)) + \ell(a)$$

while leaving all other labels unchanged,

$$d(j) = d(j) \text{ for } j \in N - \{J(a)\}$$

and modifying the tree T in an obvious fashion to contain the arc a, will produce a new labeling $(\hat{T},\hat{d})$. This observation forms the basis of the so-called *labeling methods* for finding shortest path trees. These methods employ successive *label corrections* of the above kind to construct an optimal labeling. The various labeling methods differ in their strategies for selecting arcs which are to be examined for possible label corrections.

A large class of labeling methods *branch out* from nodes, that is, they examine successively and in fixed order all arcs in the *forward star*

$$F(k) = \{a \in A\colon I(a) = K\}$$

of the node k from which to branch out. Candidate nodes for branching out are kept and prioritized on a *sequence list*. Employing a predecessor map q for characterizing trees, these methods follow the pattern:

Step 1: Put $d(r) = 0$ and $d(j) = \infty$ for $j \in N - \{r\}$.
Step 2: Enter node r into the top position of the sequence list.
Step 3: Remove the top node k from the sequence list.
Step 4: For each arc a in the forward star $F(k)$: if a violates (6), then put
$$d(J(a)) = d(I(a)) + \ell(a), \quad q(J(a)) = a,$$
and enter node $J(a)$ into the sequence list.
Step 5: If the sequence list is empty, then STOP; else return to Step 3.

Such *sequence-list driven labeling methods* are the subject of this paper. These methods differ from one another essentially in the way the nodes $J(a)$, whose labels have been corrected, are entered into the sequence list. Commonly used *sequence disciplines* that prescribe how nodes are introduced on the list include FIFO (nodes enter at the bottom), and LIFO (nodes enter at the top). There are various disciplines that are 2-WAY (nodes enter at either the bottom or top) such as the sequence discipline proposed by Pape [11]. Finally, there is the well-known discipline of DIJKSTRA (keep the sequence list sorted by labels increasing toward the bottom). We are interested in certain formal properties of such sequence disciplines.

For instance, the label $d(j)$ of some node j is called *sharp*, with respect to (T,d), if equality holds in (4). Since $d(r) = 0$ always holds for a labeling algorithm, a sharp label $d(j)$ represents the actual path length from r to j in T, and not just an upper bound. It is undesirable to branch out from a node j whose label is not sharp, since this condition guarantees that all labels directly and indirectly corrected from node j will have to be corrected again. It will be shown that LIFO and certain 2-WAY sequence disciplines branch out only from nodes having sharp labels, whereas this does not necessarily hold for a FIFO discipline. This property turns out to be closely connected to the question of how the order of nodes on the sequence list relates to the natural order of nodes in the associated tree.

2. Active Nodes

We call nodes appearing on the sequence list *active*. Since labeling methods based on sequence lists terminate when there are no active nodes remaining, the following fact is necessary for the proper functioning of such methods.

LEMMA 1: *For any sequence-list driven labeling method, the active nodes include the origins of all arcs which violate the optimality condition (6).*

PROOF: The lemma holds initially, when only the root r is active. Assume it holds at some intermediate stage. Branching out from some active node k will assure that all arcs in the forward star $F(k)$ satisfy the optimality condition. Therefore, removing node k from the sequence list will not cause the lemma to be violated. Also, the only arcs that previously satisfied (6) but do no longer must originate at those nodes whose label has been reduced by branching out from the node k. However, these nodes have just been entered in the sequence list.

LEMMA 2: *Any node* j *in* T *having a non-sharp label* d(j) *with respect to* (T,d) *must have an active ancestor in* T.

PROOF: Consider the path $P(r,j)$ in T from r to j. If all arcs in $P(r,j)$ satisfied the optimality condition (6), then

$$d(r) + l(P(r,j)) \geqslant d(j).$$

However, using property (4) of the labeling (T,d) yields

$$d(r) + l(P(r,j)) = d(j),$$

whence label $d(j)$ would in fact be sharp. Thus, at least one arc of $P(r,j)$ must violate (6), and its origin must be active by Lemma 1.

We can now derive a general condition on sequence disciplines which assures that only nodes having sharp labels are branched out from. To this end, observe that a natural order relation exists among the nodes of the tree T associated with the labeling (T,d). We write

$$i < j(T)$$

if i is an ancestor of j in T. A sequence discipline is called *order-compatible* if the sequence list never contains ancestors of the top node k in the list. In other words, the top node k does not have an active ancestor.

Examples of such sequence disciplines will be examined later in the paper. The following general condition on sequence disciplines is a direct restatement of Lemma 2.

THEOREM 1: *Under an order-compatible sequence discipline, a labeling method only branches out from nodes having sharp labels.*

3. Sequence Disciplines

As demonstrated in [2,7], the particular choice of sequence discipline employed in labeling procedures can profoundly affect the efficiency of the resulting shortest path algorithms. In this section, then, we will discuss several commonly-used sequence disciplines for determining shortest paths.

Recall that in sequence-list driven labeling methods a node is removed from the *top* of the sequence list (if the list is nonempty) and its forward star is then scanned. Any node i whose label is changed is entered, in some fashion, on the sequence list. For example, entering node i may always be placed at the *top* of the list, at the *bottom* of the list, or at *either the top or the bottom* of the list, depending on certain other information associated with node i.

In a LIFO (Last-In-First-Out) sequence discipline, any node i not appearing already on the sequence list is inserted at the top of the list. In case node i already appears on the list, either (1) the node is moved from its present list position to the top of the list, or (2) the node remains in its current position. We refer to these two variants as (1) LIFO/MOVE and (2) LIFO/NO MOVE, respectively. Shortest path algorithms based on LIFO/NO MOVE [7] make use of a "flag" to signify whether or not a node is currently on the sequence list. A reasonable implementation of the LIFO/MOVE version appears to require in addition the use of a doubly-linked list.

In a FIFO (First-In-First-Out) sequence discipline, any node i not appearing already on the list is inserted at the bottom of the list. In case node i already appears on the list, either (1) the node is moved to the bottom of the list, or (2) the node remains in its current position. Thus, in the latter case, nodes are branched out from in the order in which they are placed on the sequence list. These variants are referred to as FIFO/MOVE and FIFO/NO MOVE, respectively. The computational behavior of the second of these two variants has been studied in [2,7,8].

In the 2-WAY sequence discipline described by Pape [11], nodes i that have their label $d(i)$ corrected for the first time are placed at the bottom of the list. Nodes i that have previously been on the list (but are not currently) are placed at the top of the list when $d(i)$ is corrected. If node i already appears on the list, either (1) the node is moved from its present list position to the top of the list, or (2) the node remains in its current position. Again, these variants are referred to as PAPE/MOVE and PAPE/NO MOVE, respectively. Pape's description of this algorithm [11] leaves open which variant he has in mind. Dial, Glover, Karney, and Klingman [2] have implemented the second variant.

(In the sequence disciplines described above, the sequence list is considered to be linearly ordered, with the top node being the "first" node with respect to this linear order. If no new nodes are added to the top of the list, then the "second" node in the order thus becomes the new top node. It is easy to think of disciplines in which the associated list does not maintain a linear order structure; in these cases, the succession problem is regulated in some other manner.)

It should be noted that both the LIFO and PAPE sequence disciplines are special cases of another conceptually useful sequence discipline. Indeed, suppose f is a *tree function* defined with respect to the tree T of labeling (T,d). Namely, $f: N \to R \cup \{\infty\}$ is such that

$$i < j(T) \text{ implies that } f(i) \leqslant f(j). \tag{7}$$

If strict inequality holds above then f is called a *strict tree* function. Examples of tree functions abound. For example, if $f(i)$ denotes the number of nodes in the path $P(r,i)$ from r to i in T, then f is a (strict) tree function. Or, if $g(i)$ denotes the number of nodes in $B(i,T)$, then $-g$ is a (strict) tree function. If the network arc lengths are all nonnegative and (T,d) is a labeling, then the labels $d(i)$ define a tree function, in view of property (3). Tree functions find application in the efficient tracing of cycles in networks [1,12,13].

Consider now the *tree-derived sequence discipline,* based on a tree function f, that adds node i to the top of the list if

$$f(i) \leqslant \max \{f(u): u \text{ is active}\} \tag{8}$$

and to the bottom of the list otherwise. Here the tree function f is defined with respect to the "old" tree T prior to update by the branching out that has just corrected the label on node i. Also, we suppose that the active nodes u in (8) are those which are active in the "old" sequence list. Of course, this tree-derived sequence discipline also has two variants (MOVE/NO MOVE) depending on whether a node i already on the list is moved in the prescribed manner or remains in its current position.

Using the tree function

$$f(i) = 0 \text{ for all } i \varepsilon N$$

clearly produces the LIFO discipline. Using the tree function

$$f(i) = \begin{cases} 0 \text{ if } i \varepsilon T \\ \infty \text{ if } i \varepsilon T \end{cases}$$

produces the PAPE discipline. It will become clear later that FIFO cannot be derived from a tree function. The more general notion of a tree-derived sequence discipline has been introduced because it will be shown in the next section that every such discipline possesses the desirable property of being order-compatible.

Strict tree functions can be used to define sequence disciplines in which the top element is an active node for which the strict tree function assumes its minimum value. Such sequence disciplines are trivially order-compatible, since any active ancestor j of the current top node k would have $f(j) < f(k)$; this contradicts the fact that k was chosen to have minimum value of $f(i)$ over active nodes i. Thus, the corresponding labeling methods will automatically branch out from sharp labels, by Theorem 1.

By using the labels $d(i)$ as a tree function and selecting the top node as an active node of minimum label, one obtains the well-known "label-setting" method of Dijkstra [3], for networks with positive arc lengths. The requirement of positive arc lengths ensures that d is a strict tree function (yielding order-compatibility) and that once a node is removed from the sequence list, it will never reappear on the list (whence the label can be permanently set). Dijkstra's method also works, perhaps with minor modification, in the presence of negative arc lengths [4,10], even though the above two properties are not assured. Somewhat surprisingly, the DIJKSTRA sequence discipline is order-compatible even in the presence of negative arc lengths, as will be shown in the next section.

4. Branching Out From Sharp Labels

In this section, we present some major results that indicate which of the sequence disciplines discussed in section 3 do in fact guarantee that only nodes with sharp labels are used for branching out. This desirable property will be assured for order-compatible sequence disciplines, by Theorem 1. The first major result of this section shows that tree-derived sequence disciplines always possess this property.

THEOREM 2: *Every tree-derived sequence discipline is order-compatible.*

PROOF: Suppose the sequence discipline is not order-compatible. Then there is a first time that order-compatibility is violated. Let k be the corresponding top node of the list Λ at that time and let j be an active node ($j \varepsilon \Lambda$) such that $j < k$ (T) in the associated tree T. Since j is currently active, but has not always been active, there exists a progression of lists $\Lambda_1, \Lambda_2, \ldots, \Lambda_s$ (with associated trees $T_1, T_2, \ldots, T_s$) such that $\Lambda_s = \Lambda$, $j \varepsilon \Lambda_1$, and $j \varepsilon \Lambda_m$ for $1 < m \leqslant s$. Also, $T_s = T$.

Since node j has not been branched out from while on lists $\Lambda_1, \ldots, \Lambda_s$, it follows that

$$B(j, T_1) \supseteq B(j, T_2) \supseteq \ldots \supseteq B(j, T_s). \tag{9}$$

Indeed, the only way the branch $B(j, T_m)$ can gain new arcs in $B(j, T_{m+1})$, $1 \leqslant m < s$, is if some node $i \in B(j, T_m)$ has been branched out from. The existence of such a node $i \in \Lambda_m$ with $j < i\,(T_m)$ and $m < s$ contradicts the fact that (T_s, Λ_s) was the first instance when order-compatibility was violated.

In view of (9), the assumed relation $j < k\,(T)$ implies

$$j < k\,(T_m), \text{ for } 1 \leqslant m \leqslant s. \tag{10}$$

Moreover, it is claimed that

$$d(k) \text{ remains the same in all trees } T_1, \ldots, T_s. \tag{11}$$

Suppose, to the contrary, that $d(k)$ was corrected in branching out from node $i \in \Lambda_v$. If $i \in B(j, T_v)$, then (10) would not hold in T_{v+1}. Thus, $i \in B(j, T_v)$ with $v < s$, but this contradicts the fact that the first violation of order-compatibility occurred for (T_s, Λ_s).

Consider now the manner in which node j was added to the sequence list Λ_1.

CASE I: Node j was added to the top of Λ_1. Thus, the only way node k can precede j on list Λ_s is for $d(k)$ to have been corrected in some T_m, $1 \leqslant m \leqslant s$, contradicting (11).

CASE II: Node j was added to the bottom of Λ_1. Since k is in $\Lambda_s = \Lambda$, it must be in all Λ_m $(1 \leqslant m \leqslant s)$. Otherwise, in changing from inactive to active status at some list Λ_m, its label must have been corrected; but this is prohibited by (11). In particular, $k \in \Lambda_1$. Recall that a tree-derived sequence discipline adds node j to the bottom of list Λ_1 only if (8) fails to hold. Since $k \in \Lambda_1$, this means that $f(j) > f(k)$ in T_1. However, by (10) we have $j < k\,(T_1)$, and using property (7) of a tree-function produces $f(j) \leqslant f(k)$, a contradiction.

Since either case yields a contradiction, the sequence discipline is in fact order-compatible.

Because LIFO and PAPE sequence disciplines are special cases of tree-derived sequence disciplines, Theorems 1 and 2 produce the following results.

RESULT 1. Under LIFO/MOVE or LIFO/NO MOVE sequence disciplines, a labeling method always branches out from nodes having sharp labels.

RESULT 2. Under PAPE/MOVE or PAPE/NO MOVE sequence disciplines, a labeling method always branches out from nodes having sharp labels.

While the definition of a tree-derived sequence discipline in section 3 used a tree function f_T on the "old" tree T (before branching out has occurred), it is also possible to employ instead a tree function $f_{\hat{T}}$ based on the "new" tree $\hat{T}$ (which possibly incorporates new arcs emanating from the node just used for branching out). The proof of Theorem 2 shows that this second type of tree-derived sequence discipline is order-compatible as well. Specifically, in case II we would have $k \in \Lambda_2$, and $f(j) > f(k)$ would hold in $T_2 = \hat{T}$; again, a contradiction is reached to the fact that $j < k\,(T_2)$.

In summary, it does not really matter whether the old tree function values $f_T(i)$ or the newly-updated tree function values $f_{\hat{T}}(i)$ are used in defining the 2-WAY sequence discipline based on (8). In either case, the sequence discipline is order-compatible, and so only nodes k with sharp labels will be used for branching out. This property still holds whether we view all nodes updated by branching out as entering the sequence list simultaneously or sequentially.

However, under a FIFO sequence discipline, a node with a non-sharp label can be branched out from. For example, consider the network of figure 1, together with the associated sequence lists and trees produced an appropriate FIFO discipline. At the fourth step, node c is the top node of the list but it has an ancestor currently on the list. Thus, the label of node c is not sharp, and c will be used for branching out at the next step.

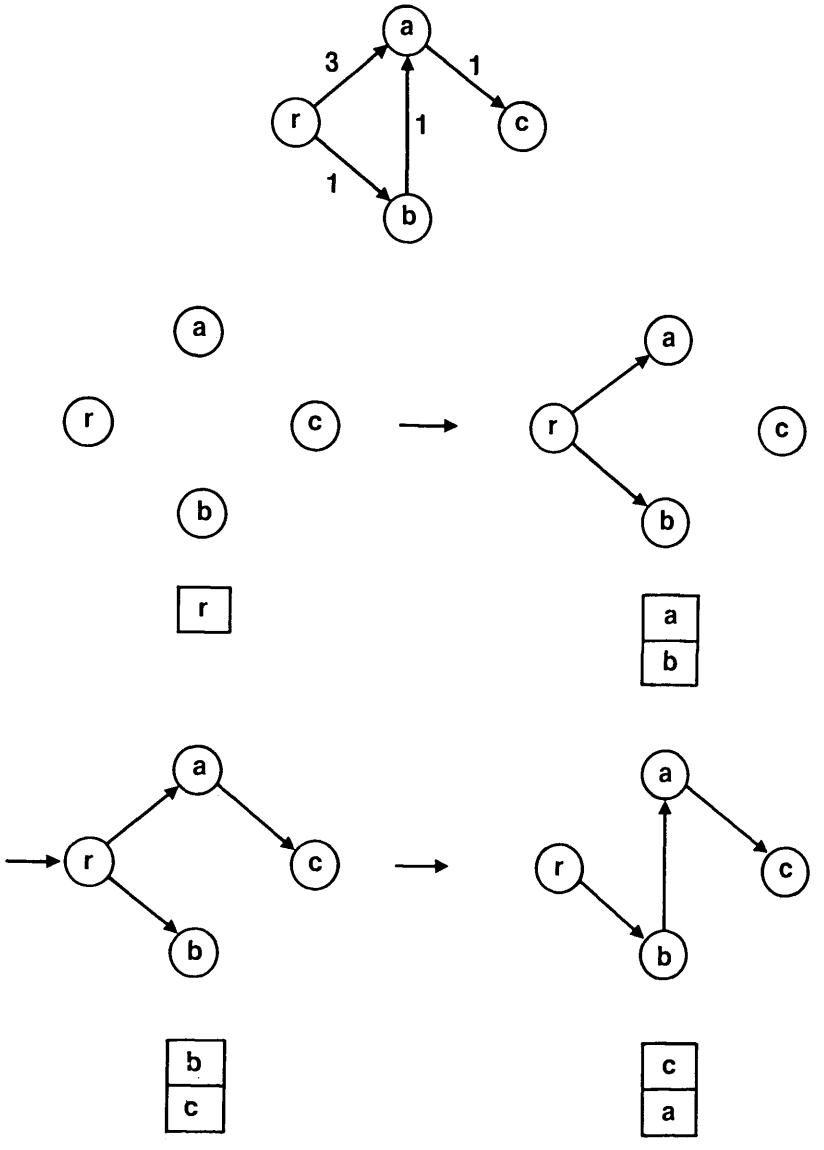

FIGURE 1.

RESULT 3. Under FIFO/MOVE or FIFO/NO MOVE sequence disciplines, a labeling method will not necessarily branch out from nodes having sharp labels.

A few additional observations are warranted. In the proof of Theorem 2, the fact that k was the top node of Λ was not used in any essential way. As a result, any tree-derived sequence discipline (including LIFO and PAPE) possesses the *strong-compatibility property*:
(SCP) If the sequence list Λ is linearly ordered and if $i,j \varepsilon \Lambda$ then

$$i < j(T) \quad i \text{ precedes } j \text{ in } \Lambda.$$

Clearly, by Theorem 1, any discipline having the SCP will always branch out from nodes with sharp labels.

Also, the LIFO/MOVE sequence discipline creates a progression of trees having a very special property. Namely, any tree generated by such a discipline must have a form like that shown in figure 2, where the

associated (linearly-ordered) sequence list Λ has entries $a, b, c, \ldots, y, z$ with a the top entry and z the bottom entry. Active nodes are indicated by squares in this figure, and inactive nodes are indicated by circles. There can be any number of active nodes (possibly none) adjacent from one of the "central" inactive nodes. The circled "I" configuration signifies an arbitrary collection of subtrees, possibly empty, of inactive nodes. This special property of LIFO/MOVE can be established in a straightforward manner by induction. Note that from the structure of the tree in figure 2, it is clear that nodes $a, b, c, \ldots, y, z$ on the sequence list are always *incomparable* in the associated tree T: i.e., neither $i < j\,(T)$ nor $j < i\,(T)$ holds. This property is not guaranteed to hold, however, for other sequence disciplines.

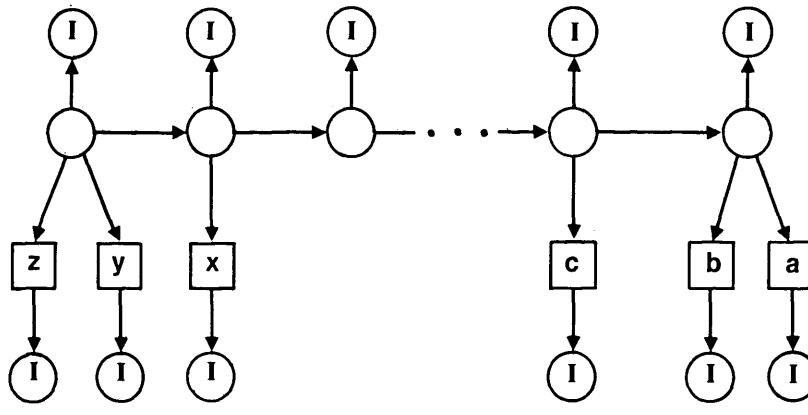

FIGURE 2.

The second major result of this section establishes that the Dijkstra sequence discipline is also order-compatible, even though arcs of negative length may be present. This result is somewhat surprising in that the labels $d(i)$ no longer form a tree function in the presence of negative arc lengths. However, it will be shown that the labels do define a tree function when restricted to active nodes (Theorem 3).

Notice that under the Dijkstra sequence discipline branching out from node k along a negative length arc creates an active label which is smaller than all labels of active nodes already on the list. Thus, the newly-labeled node becomes the top node of the list, giving the procedure somewhat the flavor of a LIFO-based procedure. To formalize this statement we define, for each node i in tree T,

$$L(i) = \min\{d(u)\colon u \text{ is active}, u \notin B(i,T)\}.$$

By convention, L(i) = ∞ if there are no active nodes outside B(i,T). Branch B(i,T) is said to be *saturated* if

$$d(j) \geq d(i)$$

holds for all active nodes j in $B(i,T)$. Our key observation is

$$L(i) \geq d(i) \text{ for nonsaturated } B(i,T). \tag{12}$$

Note that (12) implies

Each nonsaturated branch contains all active nodes of minimum label. (13)

We now proceed to prove (12). The statement is trivially satisfied for the initial labeling on the tree consisting of the root r alone. Assume it is true for subsequent labelings, including the present one (T,d,S); here S denotes the set of active nodes. After branching out from node k, which according to the modified Dijkstra procedure satisfies

$$d(k) = \min\{d(j): j \in S\},$$

a new labeling $(\hat{T}, \hat{d}, \hat{S})$ results. The nodes with actual label changes are

$$h_1, \ldots, h_m \in F(k)$$

so that

$$\hat{d}(h_t) < d(h_t), t = 1, \ldots, m,$$

$$\hat{S} = S \cup \{h_1, \ldots, h_m\} - \{k\}.$$

Note that $m = 0$ is possible. In this case, the only change is a reduction in the number of active nodes: a previously nonsaturated branch may now be saturated; $L(i)$ may increase. Statement (12) remains true regardless. We assume henceforth that $m > 0$.

CASE I: Suppose node i is not an ancestor of node k in $\hat{T}$; then it is not an ancestor of node k in T. By (13), since $B(i,T)$ does not contain the minimum node k, $B(i,T)$ is saturated in (T,d,S). Note that

$$B(i,\hat{T}) \subseteq B(i,T).$$

Moreover, any active node $j \neq i$ in $B(i,\hat{T})$ is different from $h_1, \ldots, h_m$. Thus,

$$\hat{d}(j) = d(j) \geq d(i) \geq \hat{d}(i)$$

for all active nodes $j \neq i$ in $B(i,\hat{T})$. Thus, $B(i,\hat{T})$ is saturated for all nodes $i \neq k$ which are not ancestors of k in $\hat{T}$. This implies (12) holds in $\hat{T}$ for these nodes.

CASE II: Suppose $i = k$. Then we have

$$\hat{L}(k) \geq L(k) \geq d(k) = \hat{d}(k)$$

since $B(k,T) \subseteq B(k,\hat{T})$, since there are no label changes outside $B(k,\hat{T})$, and since $d(k)$ is a minimum label in (T,d,S). This implies statement (12) holds in $\hat{T}$ for node k.

CASE III: Suppose node i is an ancestor of k in $\hat{T}$, and therefore in T. Note again that

$$B(i,\hat{T}) = B(i,T) \cup B(k,\hat{T}) \supseteq B(i,T),$$

and that there are no label changes outside $B(i,\hat{T})$. Thus,

$$\hat{L}(i) \geq L(i).$$

In addition,

$$\hat{d}(i) = d(i) \leq L(i) \leq \hat{L}(i)$$

unless $B(i,T)$ is saturated. In the latter case, since $d(k)$ is a minimum label of (T,d,S),

$$\hat{d}(i) = d(i) \leq d(k) \leq L(i) \leq \hat{L}(i).$$

Thus, (12) holds in $\hat{T}$ for all nodes.

The required result will now be shown to follow from statement (13).

THEOREM 3: *Under the DIJKSTRA sequence discipline, the labels* d(i) *form a strict tree function when restricted to the active nodes.*

REMARK. If this theorem is proved, then the DIJKSTRA discipline is order-compatible, since an active ancestor j of node k in T would by Theorem 3 satisfy $d(j) < d(k)$, contradicting the fact that node k is an active node of minimum label. We proceed therefore to a proof of the theorem.

PROOF: The theorem clearly holds for the initial labeling on the tree consisting of node r alone. Suppose the theorem holds for (T,d) and that node k is used for branching out. By induction, node k does not have an active ancestor. The only possible violation of the theorem for the next labeling $(\hat{T},\hat{d})$ occurs because a newly-active node h_t has a label that is too large. However, $B(h_t,T)$ does not contain node k and so it does not contain all active nodes with minimum label. By (13), branch $B(h_t,T)$ is saturated, whence

$$d(h_t) \leqslant d(j)$$

holds for all active nodes j in $B(h_t,T)$. Since any active node j in $B(h_t,\hat{T})$ is active in $B(h_t,T)$, and since

$$\hat{d}(h_t) < d(h_t) \leqslant d(j) = \hat{d}(j)\,,$$

all active nodes in $B(h_t,T)$ satisfy the requirements of the theorem.

RESULT 4. Under the DIJKSTRA sequence discipline, a labeling method always branches out from nodes having sharp labels.

5. Computational Complexity of Labeling Methods

In this section the (worst-case) computational complexity of labeling procedures based on various sequence disciplines will be established. We consider the effort of calculating a shortest path tree by a labeling procedure to be the number of arcs examined (i.e., used in branching out). This definition is optimistic in that it does not include the work inherent in data-structure manipulations or in finding suitable arcs to examine. For NO MOVE variants, however, the latter constitute only an insignificant portion of the total work involved. (An alternative measure of effort is the total number of nodes entered onto the sequence list. Since each such node, apart from the root, gets placed on the sequence list as a result of examining some arc, this alternative measure is a lower bound for the first.)

We first study the effort required, in the worst case, to solve the shortest path problem using a LIFO sequence discipline. Consider the networks V^n, $n = 0, 1, 2, \ldots$ defined by

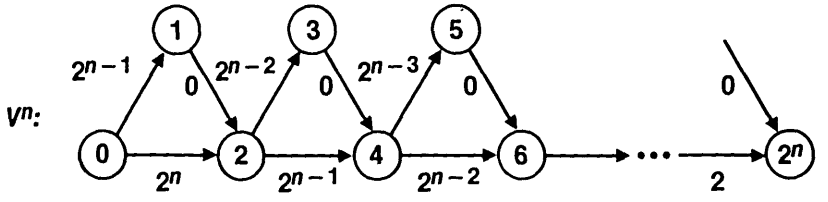

By convention, V^0 consists simply of the single node 0. Generally, V^n consists of $2n+1$ nodes and $3n$ arcs, where n designates the number of *segments*. For $n = 3$, we would have

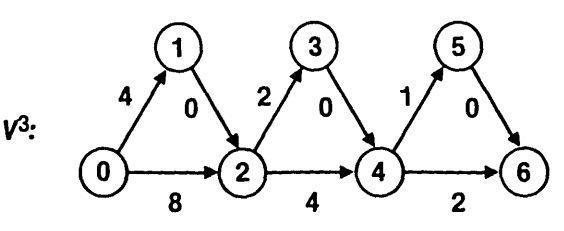

We assume further that the networks V^n are represented by forward stars and that the arcs in these forward stars are scanned in order of increasing length.

The following propositions concerning the application of LIFO to V^n follow readily by induction.

If $E(n)$ denotes the effort of solving V^n then $E(0) = 0$ and $E(n+1) = 3 + 2E(n)$ for n = 0, 1, . . . (14)

Every examination of an arc results in a node being added to the sequence list. (15)

Proposition (14) shows that $E(n) = 3(2^n-1)$ and thus the effort is exponential. Proposition (15) shows that LIFO/NO MOVE and LIFO/MOVE perform identically when applied to networks V^n. These facts are summarized in Result 5 below.

RESULT 5. Under LIFO/MOVE or LIFO/NO MOVE sequence disciplines, a labeling method has exponential computational complexity.

The idea behind the construction of the networks V^n is to build sequences of segments identical in topology, but with arc lengths for any segment being larger by a factor F than the corresponding arc lengths of the segment immediately to the right. For example, consider the networks G^n defined by

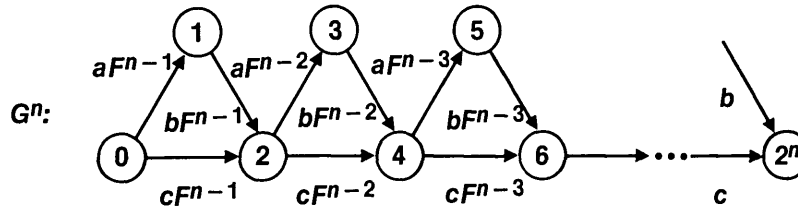

Suppose that arcs in forward stars are again scanned in order of increasing length.

LEMMA 3: *If* F ≥ 2, c > a + b, *and* c > α *then LIFO is exponential on the networks* G^n.

To show this, we first demonstrate a crucial fact about the 2^n paths from node 0 to node $2n$: $P_n(1), P_n(2), \ldots, P_n(2^n)$ which are generated by the LIFO discipline.

If paths $P_n(1), P_n(2), \ldots, P_n(2^n)$ are the paths generated in order by the LIFO discipline, then (16)

$$\ell(P_n(1)) > \ell(P_n(2)) > \ldots > \ell(P_n(2^n)).$$

PROOF: When $n = 1$, the paths are $P_1(1) = [0,2]$, $P_1(2) = [0,1,2]$ and $\ell(P_1(1)) = c > a + b = \ell(P_1(2))$, by assumption.

Suppose the assertion is true for $n = k - 1$. Then the set of paths produced in G^k by LIFO have lengths

$$\ell(P_k(1)) = F^{k-1}c + \ell(P_{k-1}(1))$$
$$\ell(P_k(2)) = F^{k-1}c + \ell(P_{k-1}(2))$$
$$\vdots$$
$$\ell(P_k(2^{k-1})) = F^{k-1}c + \ell(P_{k-1}(2^{k-1}))$$
$$\ell(P_k(2^{k-1}+1)) = F^{k-1}a + F^{k-1}b + \ell(P_{k-1}(1))$$
$$\ell(P_k(2^{k-1}+2)) = F^{k-1}a + F^{k-1}b + \ell(P_{k-1}(2))$$
$$\vdots$$
$$\ell(P_k(2^k)) = F^{k-1}a + F^{k-1}b + \ell(P_{k-1}(2^{k-1})).$$

By induction

$$\ell(P_{k-1}(1)) > \ell(P_{k-1}(2)) > \ldots > \ell(P_{k-1}(2^{k-1}))$$

and so

$$\ell(P_k(1)) > \ell(P_k(2)) > \ldots > \ell(P_k(2^{k-1})),$$

$$\ell(P_k(2^{k-1}+1)) > \ell(P_k(2^{k-1}+2)) > \ldots > \ell(P_k(2^k))$$

It suffices then to show that

$$D = \ell(P_k(2^{k-1})) - \ell(P_k(2^{k-1}+1)) > 0$$

Now,

$$D = F^{k-1}c + \ell(P_{k-1}(2^{k-1})) - (F^{k-1}a + F^{k-1}b + \ell(P_{k-1}(1)))$$

$$= F^{k-1}c + (F^{k-2}a + F^{k-2}b) + \ldots + (Fa + Fb) + (a + b) - (F^{k-1}a + F^{k-1}b + F^{k-2}c + \ldots + Fc + c)$$

$$= F^{k-1}(c-a-b) - (F^{k-2}(c-a-b) + \ldots + F(c-a-b) + (c-a-b)).$$

Since c−a−b > 0 , D > 0 if and only if

$$F^{k-1} - (F^{k-2} + \ldots + F + 1) > 0$$

or, since F > 1,

$$F^k > 2F^{k-1} - 1 .$$

Now since $F \geq 2$, $F^k \geq 2F^{k-1} > 2F^{k-1} - 1$ and so (16) is established. (In fact, $D > 0$ for all k if and only if $F \geq 2$.)

From (16) it follows that every arc incident to node 2n causes an update of d(2n), and similarly for nodes 2j ($1 \leq j < n$) and nodes 2j−1 ($1 \leq j < n$). This means all potential label corrections are made, and the exponential behavior follows with

$$E(n) = 3(2^n - 1) , n = 0, 1, \ldots$$

A similar fact holds when forward stars are ordered by decreasing length.

LEMMA 4: *If* F ≥ 2, c > a + b, *and* a > c *then LIFO is exponential on the networks* G^n.

Notice that V^n is the special case of G^n with $a = 1$, $b = 0$, $c = 2$, and $F + 2$. Lemma 3 thus guarantees exponential behavior on V^n, assuming that arcs in $F(k)$ are ordered by increasing length. The following networks W^n (corresponding to $a = 0$, $b = -2$, $c = -1$, $F = 2$) require exponential effort by LIFO when arcs in $F(k)$ are ordered by decreasing length (see Lemma 4).

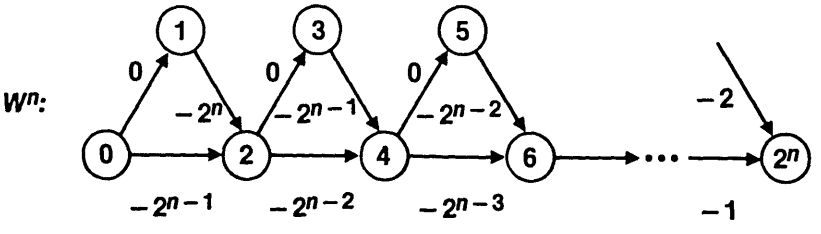

We now show that

RESULT 6. Under PAPE/MOVE or PAPE/NO MOVE sequence disciplines, a labeling method has exponential computational complexity.

This result is not surprising inasmuch as Pape's method becomes a LIFO method once all nodes have been entered on the sequence list. To exhibit an actual example, we modify networks V^n by adding arcs from the root node 0 to all nodes not already connected to it. These arcs are given a very large arc length M ($>2^{n+1}$). The forward star of the root is arranged by nonincreasing arc length, whereas all other forward stars are arranged as before by increasing arc length. Pape's method, when applied to these modified networks $\hat{V}^n$, will enter all non-root nodes into the sequence list with nodes 2 and 1 being next-to-last and last, respectively. The nodes j having label $d(j) = M$ will be branched out from first. This will not produce any label changes, so that finally all active nodes will have disappeared except nodes 2 and 1, in this order. From this point on, Pape's method will reproduce LIFO as applied to the original networks V^n. Again, there is no difference between PAPE/MOVE and PAPE/NO MOVE.

RESULT 7. Under the DIJKSTRA sequence discipline, a labeling method has exponential computational complexity if arcs of negative lengths are admitted.

This result has been previously obtained by Johnson [9]. We show that it follows rather easily from our present results. If all arc lengths are nonpositive, and if the forward stars of the network are arranged in order of decreasing arc length, then the LIFO/MOVE discipline will be equivalent to the DIJKSTRA discipline, since branching out from a node of smallest label will place another node of smallest label in the top position of the sequence list. The networks W^n described earlier then provide the necessary evidence.

RESULT 8. Under FIFO/MOVE or FIFO/NO MOVE sequence disciplines, a labeling method has computational complexity $0(n^3)$, where $n = |N|$.

To demonstrate this result, let us define sets S_t, $t = 1, 2, \ldots$, as containing those nodes added in a FIFO manner to the sequence list during branching out of nodes in S_{t-1}. We set $S_0 = \{r\}$. In the case of FIFO/MOVE, a node j whose label is updated by branching out from $k \in S_{t-1}$ is always moved to S_t, even if node j is currently on the bottom of the sequence list.

A label $d(j)$ is said to have *cardinality* $c(j)$ if the path P corresponding to the path length $d(j)$ has precisely $c(j)$ arcs. It can be readily shown by induction that for a FIFO discipline (MOVE or NO MOVE)

$$c(j) \geq t \text{ for all nodes } j \in S_t. \tag{17}$$

As a matter of fact, $c(j) = t$ for the case of FIFO/MOVE. It follows from (17) that $S_n = \phi$ inasmuch as no shortest path length $d(j)$ on the sequence list need have $c(j) > n - 1$. Thus, all FIFO methods require at most n sets S_t before terminating. Since each set S_t can contain at most $n - 1$ nodes (node r cannot re-enter the sequence list) and since branching out from a node entails at most $n - 1$ arc examinations, the effort required is no more than $0(n^3)$. It is easy to give examples where this bound is achieved and thus a FIFO-based method has worst-case complexity $0(n^3)$, as stated in Result 8.

6. Conclusions

This paper has investigated two properties of sequence disciplines for labeling procedures: branching out from sharp labels, and worst-case computational complexity. Of the disciplines studied, only FIFO fails to branch out from sharp labels, yet only FIFO has polynomial complexity. Clearly, either of these properties alone is not sufficient to guarantee good performance in practice. For example, the LIFO discipline has been observed [2,7] to be inefficient in practice, even though it branches out from sharp labels. Also, the PAPE discipline has proven to be surprisingly successful [2] in sparse networks, even though it can require exponential effort for certain sparse networks ($\hat{V}^n$ of sect. 5).

In the highly structured sparse networks used for assessing the relative efficacy of Pape's method [2], this method does indeed act similar to a FIFO method while maintaining the sharp labeling property. We conjecture that Pape's method, as well as other 2-WAY methods, can achieve success by combining in a certain sense these two desirable, but apparently conflicting, properties. At the present writing it is not known whether there exists a polynomial labeling method that branches out from sharp labels. Even if such a method cannot be found, the 2-WAY tree-derived disciplines appear to be a promising area of further investigation. For example, it is not difficult to show that a 2-WAY method, based on using the new labels d as a tree function, performs polynomially for the networks $\hat{V}^n$ on which Pape's method is exponential.

7. References

[1] Barr, R.; Glover, F.; Klingman, D. Enhancements of spanning tree procedures for network optimization. INFOR **17**: 16-34: 1979 January.

[2] Dial, R.; Glover, F.; Karney, D.; Klingman, D. A computational analysis of alternative algorithms and labeling techniques for finding shortest path trees. Networks **9**: 215-248; 1979.

[3] Dijkstra, E. W. A note on two problems in connexion with graphs. Numer. Math. **1**: 269-271; 1959.

[4] Edmonds, J.; Karp, R. M. Theoretical improvements in algorithmic efficiency for network flow problems. J. Assoc. Comput. Mach. **19**: 248-264; 1972 April.

[5] Ford, L. R. Jr.; Fulkerson, D. R. *Flows in Networks.* Princeton, N. J.: Princeton University Press; 1962. 193 pp.

[6] Frank, H.; Frisch, I. T. *Communication, Transmission, and Transportation Networks.* Reading, Mass.: Addison-Wesley; 1971. 479 pp.

[7] Gilsinn, J.; Witzgall, C. A performance comparison of labeling algorithms for calculating shortest path trees. Nat. Bur. Stand. (U.S.) Tech. Note 772; 1973 April. 87 pp.

[8] Golden, B. Shortest-path algorithms: a comparison, Operations Research **24**, Technical Note: 1164-1168; 1976 November-December.

[9] Johnson, D. B. A note on Dijkstra's shortest path algorithm, J. Assoc. Comput. Mach. **20**: 385-388; 1973 July.

[10] Murchland, J. D. The 'once-through' method of finding all shortest distances in a graph from a single origin, London School of Economics, LBS-TNT-56.1; 1969.

[11] Pape, U. Implementation and efficiency of Moore-algorithms for the shortest route problems, Math. Programming **7**: 212-222; 1974.

[12] Shier, D. R.; Witzgall, C. Arc tolerances in shortest path and network flow problems, Networks **10**: 277-291; 1980.

[13] Srinivasan, V.; Thompson, G. L. Accelerated algorithms for labeling and relabeling of trees, with applications to distribution problems, J. Assoc. Comput. Mach. **19**: 712-726; 1972 October.

[14] Witzgall, C.; Gilsinn, J. F.; Shier, D. R. Shortest paths in graphs, in *Case Studies in Mathematical Modeling,* London: Pitman Publishing (in pess).